

# Vehicle Dynamics on Competition

*André Filipe de Castro Barbosa*

**Master's Dissertation**

FEUP Supervisor: Prof. José Ferreira Duarte

External Supervisor: Eng. Sacha Jordan



**Master in Mechanical Engineering**

September 2023

*This page was left blank purposely*

## Abstract

The dynamics of a racing vehicle represent a complex interaction between engineering prowess, scientific research, and the sheer talent of the driver. In the pursuit of victory on the racetrack or at the event, this project aims to provide a concise overview of the main aspects and importance of the dynamics of a high-performance racing vehicle, aligning its capabilities with the demands of competitive motorsport. This summary provides an overview of the project's objectives, methods and expected results.

It addresses several fundamental principles, including suspension geometry and design, mass distribution and the position of the centre of gravity, tyre grip on the road and other dynamic parameters. The objectives are to improve performance parameters, including cornering speeds, acceleration and ensuring a competitive edge in racing series. Optimising handling and stability, to achieve an ideal balance between responsiveness and control, ensuring that the vehicle responds precisely to the driver's interventions in the most demanding racing conditions. Maximising grip and traction, improving tyre performance, and optimising suspension geometry, allowing the vehicle to maintain control during cornering and high-speed braking.

The project's methodology is founded on a systematic approach that combines engineering expertise with cutting-edge technology, in an iterative development of a tool adapted to the user. This leads to the construction and development of a spreadsheet capable of calculating dynamic calculations, suspension stiffnesses and setup values. Subsequently, a thorough review of the existing data and performance metrics is carried out in order to provide further improvements and assess the impact of the proposed modifications. This way, a process of continuous improvement is carried out based on test results and driver feedback, ensuring that the project is aligned with performance objectives.

The completion of this project is expected to produce a specific racing vehicle tool that epitomises dynamic performance in racing events. In addition, the project will serve as a demonstration to the synergy between engineering innovation and the art of racing, inspiring new advances in motorsport.

As the racing vehicle dynamics project develops, it embodies the relentless pursuit of excellence that characterises the world of motorsport. The combination of technical ingenuity, precision engineering and the unwavering determination to outperform rivals is a testimony to the dedication of everyone involved. Through this project, the limits of racing vehicle dynamics will be pushed, setting a new standard of competitive excellence.

## Resumo

A dinâmica de um veículo de competição representa uma interação complexa entre a engenharia, a investigação científica e o talento do piloto. Na busca da vitória na pista de corridas ou no evento, este projeto visa fornecer uma visão concisa dos principais aspetos e da importância da dinâmica de um veículo de corrida de alto desempenho, alinhando as suas capacidades com as exigências do desporto automóvel de competição. Este resumo fornece uma visão geral dos objetivos, métodos e resultados esperados do projeto.

Engloba vários princípios fundamentais, incluindo a geometria e a conceção da suspensão, a distribuição da massa e a posição do centro de gravidade, a aderência dos pneus à estrada e outros parâmetros dinâmicos. Os objetivos são melhorar os parâmetros de desempenho, incluindo as velocidades em curva e a aceleração, e garantir uma vantagem competitiva nas séries de corridas. Otimizar o comportamento e a estabilidade, para alcançar um equilíbrio ideal entre capacidade de resposta e controlo, garantindo que o veículo responde com precisão às intervenções do condutor nas condições de corrida mais exigentes. Maximização da aderência e da tração, melhorando o desempenho dos pneus e otimizando a geometria da suspensão, permitindo que o veículo mantenha o controlo durante as curvas e as travagens a alta velocidade.

A metodologia do projeto baseia-se numa abordagem sistemática que combina conhecimentos de engenharia com tecnologia de ponta, num desenvolvimento iterativo de uma ferramenta adaptada ao utilizador. Esta, por sua vez, leva à construção e desenvolvimento de uma folha de cálculo capaz de calcular cálculos dinâmicos, rigidez da suspensão e valores de configuração. Posteriormente, é efetuada uma revisão exaustiva dos dados existentes e das métricas de desempenho, de forma a proporcionar mais melhorias e avaliar o impacto das modificações propostas. Desta forma, é executado um processo de melhoria contínua com base nos resultados dos testes e no feedback dos condutores, assegurando o alinhamento do projeto com os objetivos de desempenho.

Espera-se que a conclusão deste projeto produza uma ferramenta específica para veículos de corrida que simbolize o desempenho dinâmico nos respetivos eventos de corrida. Além disso, o projeto servirá de testemunho da sinergia entre a inovação da engenharia e a arte das corridas, inspirando novos avanços no desporto automóvel.

À medida que o projeto de dinâmica de veículos de competição se desenvolve, incorpora a busca incessante da excelência que caracteriza o mundo dos desportos motorizados. A combinação de engenho técnico, engenharia de precisão e a determinação inabalável de superar os rivais é um testemunho da dedicação de todos os envolvidos. Através deste projeto, os limites da dinâmica dos veículos de competição serão ultrapassados, estabelecendo um novo padrão de excelência competitiva.

## Acknowledgments

Although a dissertation is essentially an individual piece of work, there are contributions that should not be overlooked, and it is also the culmination of five years of dedication, effort, and resilience.

I would like to express my sincere gratitude to the following people and institutions without whose support, guidance, and encouragement the completion of this dissertation would not have been possible:

**Academic Advisors and Mentors:** Professor José Ferreira Duarte and Engineer Sacha Jordan - Your unwavering support, invaluable guidance and expertise in vehicle dynamics were fundamental in shaping this research. The constructive feedback is aimed at the quality and rigour of this project.

**Internship Organisation:** I would like to thank The Racing Factory and its CEO Aloísio Monteiro for their support during my internship, which enabled me to carry out my research and complete this dissertation.

**Friends and Colleagues:** I am grateful to my friends who have provided me with support, camaraderie, and insightful discussions throughout this journey. Your friendship and intellectual exchange have enriched my academic experience. Namely Guilherme Outeiro, Mariana Costa for their invaluable contribution to this dissertation.

**Family:** To my family, your endless encouragement, and belief in my abilities have been my greatest motivation throughout this academic journey. Your sacrifices and understanding during the nights and weekends dedicated to research are deeply appreciated.

**Participants and Interviewees:** My thanks to the participants and interviewees who generously shared their time and ideas for this research.

**Educational Institution:** I would like to thank the Faculty of Engineering of the University of Porto, FEUP, for providing a favourable academic environment, access to resources and a platform for intellectual growth. And gratitude to all the Professors who shared their knowledge and experience during this journey that I will carry with me into the future.

I apologise if I have inadvertently omitted anyone, as your contributions have been numerous and deeply appreciated. This dissertation is the culmination of collective efforts, and I am grateful for the support of each and every one of you.

# Table of Contents

1	Introduction.....	1
1.1	Context and motivation.....	1
1.2	Vehicle Dynamic on The Racing Factory .....	1
1.3	Project objectives .....	2
1.4	Methodology.....	2
1.5	Structure of the Dissertation.....	3
2	Literature Review .....	4
2.1	Vehicle System .....	4
2.1.1	Coordinate System .....	4
2.1.2	Axis.....	4
2.1.3	Angles.....	5
2.2	Suspension Geometry.....	6
2.3	Vehicle Dynamics.....	7
2.3.1	Sprung Mass and Unsprung Mass.....	8
2.4	Tyre Behaviour.....	8
2.4.1	Wheel Coordinate System .....	8
2.4.2	Tyre contact patch or Footprint .....	9
2.4.3	Grip.....	9
2.4.4	Tyre Pressure .....	9
2.4.5	Temperature .....	10
2.4.6	Tyre compound.....	10
2.4.7	Slip Angle.....	10
2.4.8	Lateral Force.....	12
2.4.9	Longitudinal Force .....	13
2.4.10	Braking Force .....	13
2.4.11	Tractive Condition.....	14
2.4.12	Longitudinal Slip Ratio .....	14
2.4.13	Vertical Force.....	15
2.4.14	Aligning Torque.....	16
2.4.15	Rolling Resistance .....	16
2.4.16	Friction Circle and Ellipse .....	16
2.5	Wheel Alignment .....	18
2.5.1	Camber.....	18
2.5.2	Camber Thrust.....	19
2.5.3	Caster Angle.....	20
2.5.4	Ackermann Steering Geometry.....	20
2.5.5	Toe.....	21
2.6	Centre of Gravity, CG.....	22
2.7	Instantaneous Centre .....	22
2.8	Roll Centre .....	23
2.9	Anti-Dive.....	24
2.10	Anti-Squat .....	25
2.11	Springs.....	26
2.12	Dampers.....	28
2.13	Vibration System and Damper .....	30
2.14	Anti-roll bar.....	33
3	Mathematic Modulation .....	36
3.1	Location x and y of the CG.....	38
3.2	Vertical Location of the CG .....	39
3.3	Sprung Mass CG Location .....	40
3.3.1	Location x and y of sprung mass CG .....	40

3.3.2	Vertical Location of sprung mass CG.....	41
3.4	Excel – Centre of Gravity .....	42
3.5	Roll Rates.....	43
3.6	Excel – Mechanical Balance .....	45
3.7	Wheel Load under constant Braking .....	46
3.8	Wheel Loads Under Cornering.....	47
3.9	Excel – Weight Transfer .....	48
4	Procedure and Solution.....	50
4.1	Previous Vehicles Analyses .....	50
4.2	Mass Distribution.....	50
4.2.1	Horizontal Centre of Gravity.....	53
4.2.2	Vertical Centre of Gravity.....	53
4.3	Instantaneous centre and roll centre .....	54
4.4	Ride and Roll Characteristics .....	57
4.4.1	Springs Characteristics .....	57
4.4.2	Anti-roll Bar Characteristics .....	58
4.5	Mechanical Balance .....	61
4.6	System Response Analysis.....	62
4.7	Data Analysis .....	63
4.7.1	Wintax4 – 4.80.....	64
4.7.2	Analysing Data.....	64
4.7.3	Driving Data .....	65
5	Conclusion and Recommendations .....	68
	References .....	70
	ANNEXE A:Data from Skoda .....	71
	ANNEXE B:Worksheet .....	72
	ANNEXE C:Recording Measurements.....	73

## Glossary

**ISO** – International Organisation for Standardisation

**SAE** – Society of Automotive Engineering

**FIA** – Federation Internationale de l'Automobile

**CG** – Centre of gravity

$\psi$  – Yaw or heading angle

$\alpha$  – Slip angle

$\beta$  – Attitude angle

$\delta$  – Steer angle

$l$  – Wheelbase

$a$  – Distance from front axle to centre of gravity

$b$  – Distance from rear axle to centre of gravity

$h$  – Centre of gravity height

$F_y$  – Lateral force on tyre

**SR** – Slip ratio

$M_z$  – Aligning torque

$R_k$  – Rolling resistance

$\Upsilon$  – Camber angle

$K$  – Spring stiffness

$\Delta l$  – Displacement

$c_{cr}$  – Critical damping

$c$  – Damping coefficient

$\xi$  – Damping ratio

$\Delta \dot{Z}$  – Velocity displacement

**ARB** – Anti-roll bar

$M_t$  – Torsion moment

$\theta$  – Torsion angle

$G$  – Elasticity of material

$I_p$  – Inertial polar moment

$K_\theta$  – vehicle roll rate

$K_{\theta T}$  – tyres roll rate

$K_{\theta S}$  – spring roll rate

$K_{\theta B}$  – anti-roll bar roll rate

$K_W$  – Wheel centre rate

$K_S$  – Spring rate

**IR** – Installation ratio

**CIR** – Centre instantaneous of rotation

**RC** – Roll centre

**W** – Total weight of the vehicle

$W_1$  – Front left wheel

$W_2$  – Front right wheel

$W_3$  – Rear left wheel

$W_4$  – Rear right wheel

$W_F$  – Total front weight

$W_R$  – Total rear weight



$t_F$  – Front track width  
 $t_R$  – Rear track width  
 $R_{LF}$  – Front wheel centre height above ground  
 $R_{LR}$  – Rear wheel centre height above ground  
 $W_S$  – Total sprung weight  
 $W_{UF}$  – Front unsprung weight  
 $W_{UR}$  – Rear unsprung weight  
 $W_{U1}$  – Left front wheel unsprung weight  
 $W_{U2}$  – Right front wheel unsprung weight  
 $W_{U3}$  – Left rear wheel unsprung weight  
 $W_{U4}$  – Right rear wheel unsprung weight  
 $a_S$  – Distance from front axle to centre of gravity of sprung mass  
 $b_S$  – Distance from rear axle to centre of gravity of sprung mass  
 $h_S$  – Centrer of gravity of sprung mass

## Figures Index

Figure 1 - The Racing Factory company logo .....	1
Figure 2 - Gantt's diagram of tasks of the project .....	3
Figure 3 – Vehicle coordinate system, ISO 8855:2011 .....	4
Figure 4 - Vehicle axis system, ISO 8855-2011 .....	5
Figure 5 - Representation of heading, sideslip, and steer angle (William F. Milliken 1995) ....	5
Figure 6 - Different suspension geometry (Baylos 2016) .....	6
Figure 7 - Installation ratio (William F. Milliken 1995) .....	7
Figure 8 - Forces and moments (Rajamani 2005) .....	9
Figure 9 - Effect of tyre pressure on contact patch (Balkwill 2018d) .....	10
Figure 10 - Effect of temperature on grip (Balkwill 2018d) .....	10
Figure 11 - Schematic of slip angle (Balkwill 2018d).....	11
Figure 12 - Slip angle vs lateral force (William F. Milliken 1995).....	12
Figure 13 - Slip angle vs lateral force coefficient (William F. Milliken 1995).....	13
Figure 14 – Brush model for braking (Balkwill 2018d).....	14
Figure 16 - Braking behavior curve, slip angle = 0° (William F. Milliken 1995).....	15
Figure 15 - Traction behavior curve, slip angle = 0° (William F. Milliken 1995) .....	15
Figure 17 - Coefficient of friction vs vertical load (Balkwill 2018d) .....	15
Figure 18 - Lateral force vs vertical load (Balkwill 2018d).....	15
Figure 19 - Rolling resistance in tractive torque (Balkwill 2018d).....	16
Figure 20 - Tyres forces through one corner (Balkwill 2018b).....	17
Figure 21 - Friction circle (Balkwill 2018b) .....	17
Figure 22 - Positive and negative camber, respectively (vehicle dynamics, 2006).....	18
Figure 23 - Temperature measurement points on a tarmac tyre (Michelin 2001).....	19
Figure 24 - Example of too much camber on tarmac tyre (Michelin 2001).....	19
Figure 25 - Camber thrust (Balkwill 2018d) .....	19
Figure 26 - Caster angle (Crahan 2023) .....	20
Figure 27 - Ackermann steering geometry principle (Smith 1978).....	20
Figure 28 - Different steering geometry (a) parallel, (b) ackermann and (c) reverse ackermann (Balkwill 2018b).....	21
Figure 29 - Definition of toe (Guiggiani 2018) .....	21
Figure 30 - Centre of gravity (Beckam 1991) .....	22
Figure 31 - Representation of Instantaneous Centre (William F. Milliken 1995).....	22
Figure 32 - Instantaneous centre in MacPherson suspension, front view (Rio 2009).....	23
Figure 33 - Instantaneous centre MacPherson in front (left side) and side view (right side) (William F. Milliken 1995) .....	23

Figure 34 - Representation of roll centre in symmetric (a) and asymmetric (b) suspension geometry (William F. Milliken 1995) .....	24
Figure 35 - Roll centre (RC) in MacPherson suspension (Ferreira 2023).....	24
Figure 36 - Anti-Dive free body (William F. Milliken 1995) .....	24
Figure 37 - Anti-Squat geometry.....	25
Figure 38 - Helical coil springs (William F. Milliken 1995) .....	26
Figure 39 - Digital coil spring tester from Intercomp ("Intercomp") .....	27
Figure 40 - Coil Spring Stiffness graphs of the recorded values.....	27
Figure 41 - Damper assembly on Skoda Fabia R5 (Skoda_Motorsport 2023b) .....	28
Figure 42 - Damper setting (Skoda_Motorsport 2023b) .....	28
Figure 43 - Damper force vs displacement curve (Seward 2014) .....	29
Figure 44 - Handling corner sections (Kasprzak 2012).....	29
Figure 45 - Underdamped (blue), critically damped (green) and overdamped (red) analysis for response to step steer (Balkwill 2018c).....	30
Figure 46 - System response to critical damping (Rodrigues 2021) .....	31
Figure 47 - Spring mass damper system response (Catto 2012) .....	31
Figure 48 - One corner of the vehicle (right) and the transmissibility of unsprung mass (left) (William F. Milliken 1995) .....	32
Figure 49 - Damping on curve for good and poor roadway (William F. Milliken 1995) .....	32
Figure 50 - Understeer vs. Oversteer (Bugeja, Spina, and Buhagiar 2017) .....	33
Figure 51 – Anti-roll bar geometry at Skoda (Skoda_Motorsport 2023b).....	33
Figure 52 - Adjust system of anti-roll bar (Skoda_Motorsport 2023b).....	34
Figure 53 - Theta variation at distinct positions of drop link (Skoda_Motorsport 2023b) .....	34
Figure 54 - Excel spreadsheet of input data .....	36
Figure 55 - CG spreadsheet Excel, part of the information section .....	37
Figure 56 - Spring spreadsheet Excel, part of the information section .....	37
Figure 57 - Centre of gravity location on x and y (William F. Milliken 1995).....	38
Figure 58 - Vertical location of centre of gravity (William F. Milliken 1995).....	39
Figure 59 - Sprung mass CG location, <i>WS</i> (William F. Milliken 1995).....	40
Figure 60 - Height of sprung mass centre of gravity (William F. Milliken 1995) .....	41
Figure 61 - Excel spreadsheet, Centre of Gravity .....	42
Figure 62 - Excel spreadsheet, Centre of Gravity - Roll centre height calculation.....	43
Figure 63 - Wishbone ratio.....	45
Figure 64 - Excel spreadsheet, Mechanical Balance .....	46
Figure 65 - Free-body diagram for acceleration(Balkwill 2018a).....	46
Figure 66 - Free body diagram on cornering (Balkwill 2018b) .....	47
Figure 67 - Excel spreadsheet, Weight Transfer .....	49

Figure 68 - Weight transfer graphic .....	49
Figure 69 - Platforms with scales to create the plan ground .....	51
Figure 70 - Weight of car, with guards and ballast .....	52
Figure 71 - Weight with driver and co-driver .....	52
Figure 72 - Weight with addition of 35L of fuel .....	52
Figure 73 - Weight with addition of second spare tyre .....	52
Figure 74 - Elevation of the vehicle .....	54
Figure 75 - Scheme of suspension measures .....	55
Figure 76 - Suspension elements and measure process .....	55
Figure 77 – Anti-Roll torque for tarmac springs .....	57
Figure 78 - Wheel rate graphic for tarmac springs .....	58
Figure 79 - Frequency for the tarmac springs.....	58
Figure 80 - Front ARB for the different diameters and positions .....	59
Figure 81 - Rear ARB for the different diameters and positions .....	60
Figure 82 - Part of the cover tab at Excel software .....	61
Figure 83 - Part of the mechanical balance tab at Excel software.....	62
Figure 85 - System response for damping ratio of 1 .....	63
Figure 84 - System response for damping ratio 0,75.....	63
Figure 86 - Wintax software interface .....	64
Figure 87 - Acquisition manager on Wintax .....	64
Figure 88 - Acquisition tab on Wintax .....	64
Figure 89 - Interface with data for analyse in one stage.....	65
Figure 90 - Interface driving analyses .....	66
Figure 91 - Correction on the driving.....	66
Figure 92 - Comparation of data of two test runs.....	67
Figure 93 - Excel cover spreadsheet.....	72
Figure 94 - Measurement record sheet .....	73

## Table's Index

Table 1 – Registered coil spring stiffness values .....	27
Table 2 - Effective diameter of anti-roll bar Skoda Rally2 Evo (Skoda_Motorsport 2023b) ..	34
Table 3 - Data from homologation book (Skoda_Motorsport 2023a).....	50
Table 4 - Weights considering different steps .....	52
Table 5 - Location of x and y of the centre of gravity on this specific case.....	53
Table 6 - Location of height of the centre of gravity.....	54
Table 7 - Measurement points for front roll centre .....	55
Table 8 - Suspension measures for calculation of the front roll centre height .....	56
Table 9 - Measurement points for rear roll centre .....	56
Table 10 - Suspension measures for calculation of the rear roll centre height.....	56
Table 11 - Front ARB rates for the different diameters and positions .....	59
Table 12 - Rear ARB rates for the different diameters and positions .....	59
Table 13 - Percentage increase in the torsional stiffness modulus .....	60
Table 14 - Roll distribution in ARB, with consideration front position.....	61
Table 15 - Springs available and homologated by Skoda for tarmac.....	71
Table 16 - Springs available and homologated by Skoda for gravel.....	71

# 1 Introduction

## 1.1 Context and motivation

Vehicle dynamics is a captivating field of study that investigates the intricate science behind the movement and behaviour of vehicles on the road. It is a branch of automotive engineering that seeks to understand how cars, motorbikes and other wheeled vehicles interact with the road, the environment, and the actions of the driver. By examining the forces, moments and movements involved, vehicle dynamics aims to optimise the performance, safety and driving characteristics of vehicles.

In the world of motorsport, there are some computer programmes to simulate laps or to help design the vehicle in terms of geometry, but it's difficult to find one that can be adapted for quick analysis during races. Top teams and well-supported engineers have the design of a specific brand for their individual work. In this exciting field, engineers and researchers explore the complex interaction of factors such as vehicle weight distribution, suspension design, tyre properties, aerodynamics, and control systems. In doing so, they seek to improve the stability, manoeuvrability and driving comfort of vehicles.

This project aims to create a tool that provides a basis for aspiring engineers in vehicle dynamics with some previous work in the workshop, taking into account support for future events and a gateway to a fascinating world where science, engineering and innovation converge to push the boundaries of what is possible.

## 1.2 Vehicle Dynamic on The Racing Factory

The Racing Factory is a company born in 2018, entirely dedicated to motorsport and based in S. Paio de Oleiros, in the municipal district of Santa Maria da Feira, Portugal. The company logo is shown in Figure 1.



Figure 1 - The Racing Factory company logo

It provides various services in the Motorsport area, the main ones being the following: Mechanical Preparation and Maintenance; Logistics Operations; Engineering and Development; Competition Car Rental; Motorsport Products; Communication and Design Service.

In a short period of time, they have already won several titles, including the Portuguese Rally Championship (2020 and 2022) and the Madeira Rally Championship (2020 and 2022). Of particular note is the unprecedented achievement in 2022, in Portugal, with the conquest of the CPR title in R2 and R4 in the same year.

The project was proposed to develop a simple-to-use, free-to-use tool for those working on these events, thus supporting tests and races for the most accurate solution to setup changes. There are a number of tools for analyses, but they are specific to a particular user or limited in the amount of work that can be carried out. For this purpose, creating a tool in Microsoft Excel has the advantage of being freely accessible and not requiring licences.

### 1.3 Project objectives

The main objectives of this project are multidimensional, with a theoretical understanding of the primary principles of vehicle dynamics and the practical reality of the complexity of vehicle dynamic behaviour. These objectives guide the focus of the project and help define its scope.

The first phase is a theoretical understanding of the factors that affect behaviour, the differences between geometries and the intercorrelation between these factors, in order to create the necessary bases for developing the spreadsheet with the objectives defined as:

1. Improving handling and stability: optimising vehicle dynamics for cornering, braking and high-speed acceleration, ensuring stability and control in extreme racing conditions.
2. Optimise weight distribution: Fine-tune the weight distribution to achieve the ideal balance between the front and rear axles, improving cornering performance and overall stability.
3. Reduce roll and pitch: Minimise body roll and pitch during cornering and braking, improving vehicle responsiveness and driver confidence.
4. Refine suspension setup: Adjust suspension geometry, damping and spring rates for different tracks/races and racing conditions to maximise handling and tyre contact.
5. Driver feedback: Collaborate closely with drivers to fine-tune vehicle dynamics based on their comments and preferences, creating a harmonious partnership between man and machine.
6. Competitor analysis: Continuously analysing competitor vehicles and strategies to identify areas for improvement and gain a competitive advantage.

With this theoretical basis in mind and these objectives, the aim was to create a tool with the first sheet containing all the important information to effectively make the best decision to respond to or optimise the vehicle's behaviour. And on the other sheets, in more detail, the different parameters to take into account when in-depth knowledge is required. Because there isn't just one answer or one right way, there are different alternatives and choices needed to get the best result.

### 1.4 Methodology

The methodology chapter of this dissertation gives an insight into the procedures and practices used to take the complexity of the study in the direction of good efficiency and management with the practical study. As already mentioned, since this dissertation is carried out in a company context, the initial weeks required a comprehensive understanding of the company's procedures, departments, organization and personnel.

The research begins with the organisation of information, research books on vehicle dynamics, in order to have a good basis and support for future in-depth studies and to ensure greater coverage of the complex nature of the subject. Chapter 2, Literature Review, presents the theoretical background and contextualises the understanding of the research.

An explanation of the themes and details for the development of the future tool is presented.

The spreadsheet and a practical analysis under real conditions and the presentation of vehicle telemetry data with driver comments are presented in Chapter 3 and Chapter 4.

Finally, Chapter 5 summarises and analyses the results and conclusions of the qualitative and quantitative findings. Decisions were or were not correlated with the theoretical and practical framework.

Figure 2 presents a Gantt diagram showing the schedule of tasks in relation to the time required for each task.

	Task	Deadlines							
		FEB	MAR	APR	MAY	JUNE	JULY	AUG	SEPT
Project Phases	Companie Integration								
	Problem Characterization								
	State of the art research								
	Study of Suspension System								
	Study of Vehicle Data Analyse								
	Mathematical Modeling on Excel								
	Practical realisation of the study								
	Comparasion and conclusions								
	Document Writing								

Figure 2 - Gantt's diagram of tasks of the project

### 1.5 Structure of the Dissertation

The dissertation is structured around a global understanding of the study carried out on vehicle behaviour. It is structured in five fundamental chapters, in which the themes are presented.

Chapter 1, the Introduction, briefly describes the study, the research objectives and the motivation for carrying out this research. It establishes a starting point for the future presentation of the research.

Chapter 2, Literature Review, presents a theoretical basis for a comprehensive understanding of the project. It introduces the principles for a basic and in-depth understanding of the concepts. This chapter basically creates a context for the following two analysis chapters.

Chapter 3, presents the calculations and explains how they are used in the construction of the spreadsheets.

Chapter 4, then shows the results of the practical application of the tool by presenting telemetry data from the vehicle together with comments from the driver on the behaviour and sensation of the respective changes.

Finally, Chapter 5, concludes all the work carried out in the previous chapters and recommends improvements that can be made closer to real behaviour in order to make the best decisions.

All the chapters together form a cohesive and comprehensive narrative that combines theoretical understanding with practical application of the complexity of vehicle behaviour.



## 2 Literature Review

### 2.1 Vehicle System

For vehicle performance, it is necessary to start by defining the axis systems to which the variables can refer, for example speed, acceleration, external forces, and others acting on the vehicle.

#### 2.1.1 Coordinate System

The coordinate system used is an important reference for use in the more complex topics discussed below. In the automotive industry, two references are used, namely ISO 8085 (International Organisation for Standardisation, 2011) and SAE J676e (Society of Automotive Engineers, 2008).

Throughout this work, the ISO 8055 coordinate diagram shown in Figure 3 will be used.

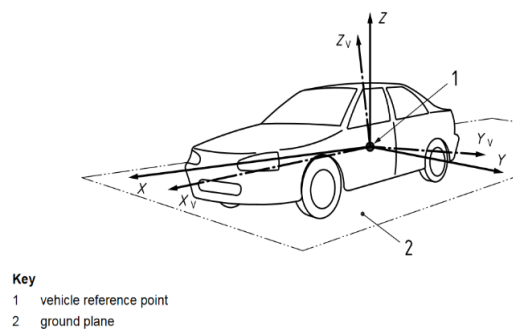


Figure 3 – Vehicle coordinate system, ISO 8855:2011

In Figure 3, the vehicle's reference point is labelled 1 and ground plane is labelled 2. A system of axes is attached to the vehicle's sprung mass (explained in more detail in point 2.3.1 Sprung Mass and Unsprung Mass), with the  $X_v$  axis horizontal and forward and parallel to the vehicle's longitudinal plane of symmetry, the  $Y_v$  axis perpendicular to the vehicle's longitudinal plane and pointing positively to the left, and the  $Z_v$  axis pointing upwards. The non-reference axis has the same reference point, but the orientation in relation to the ground has been fixed.

Figure 4 shows the multiple spatial degrees of freedom, 3 translations and 3 rotations.

#### 2.1.2 Axis

The axis is used as a coordinate system to describe the three-dimensional movement and orientation of a vehicle. This coordinate system helps to analyse various aspects of a vehicle's behaviour, including its motion, forces, and stability.

**X axis:** translation occurs in the direction of the travel with velocity  $V_x$  and longitudinal acceleration. Rotation around the X axis is called **Roll** and is the result of lateral acceleration. It results from a force arm between the CG (centre of gravity) and the roll axis. Roll occurs when a vehicle leans to one side and is usually observed during a corner, when the vehicle leans to the outside of the corner.

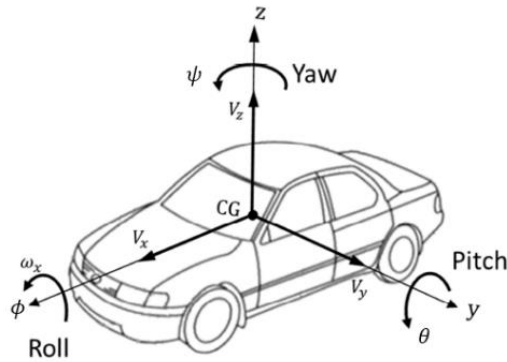


Figure 4 - Vehicle axis system, ISO 8855-2011

**Y axis:** the translation cannot roll freely as in the X axis, longitudinal direction, but results from the vehicle's slip angle, dealt with later in the point 2.4.7. Rotation, known as **Pitch** or dive, occurs during longitudinal acceleration, due to a force arm between the centre of gravity and the nodal axis. Pitch occurs when the nose and tail of a vehicle move up and down and is normally observed during acceleration and braking.

**Z axis:** translation in the Z direction has the velocity  $V_z$  and is the Normal acceleration. In terms of rotation around the Z axis, it is called **Yaw** since the vehicle rotates around its vertical axis. This movement is observed when the vehicle changes direction, for example during steering manoeuvres.

### 2.1.3 Angles

In vehicle control, heading, sideslip and steering angle are concepts that describe different aspects of a vehicle's orientation and movement. These parameters are necessary to understand the behaviour of a vehicle and how it reacts to driver actions and external forces.

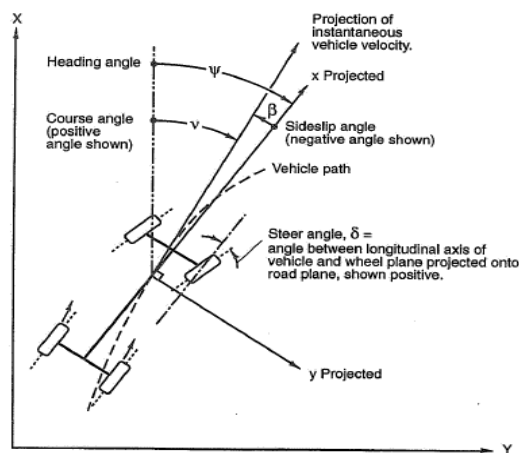


Figure 5 - Representation of heading, sideslip, and steer angle (William F. Milliken 1995)

**Heading Angle,  $\Psi$ :** is the angle between the trace in the X-Y plane of the vehicle's x-axis and the Earth's fixed axis system. It refers to the orientation or direction in which a vehicle is pointed.

**Sideslip angle,  $\alpha$  (Attitude angle,  $\beta$ ):** is the angle between the trace in the X-Y plane of the vehicle's x-axis and the vehicle's velocity vector at a specified point. It represents the

difference between the direction in which a vehicle is moving and the direction in which the vehicle is pointed.

**Steering Angle,  $\delta$ :** is the angle between the longitudinal axis of the vehicle and the plane of the wheel projected onto the plane of the road. It refers to the angle of turn of the front wheels in relation to the longitudinal axis of the vehicle, which quantifies the degree to which the driver has turned the steering wheel.

## 2.2 Suspension Geometry

The connection between the sprung mass and the unsprung mass of a vehicle is made by suspension elements that are related to suspension geometry. Suspension geometry controls how the transmission of forces between the two masses takes place and controls the trajectory of the relative movement of the wheel. There are numerous suspension geometry designs, each with its own advantages and disadvantages, which means that there is no single best geometry, and each is specific to the needs of the vehicle, Figure 6. The different types of suspension geometry are also related to the possible leverage effect that comes from them. Looking at Figure 6, it is possible to see the variation of the anchor point ‘C’ in different solutions in different types of constructive geometries of the suspension geometry of a vehicle, for example, if the mechanical advantage is high, it means that the wheel rate is much lower than the spring rate.

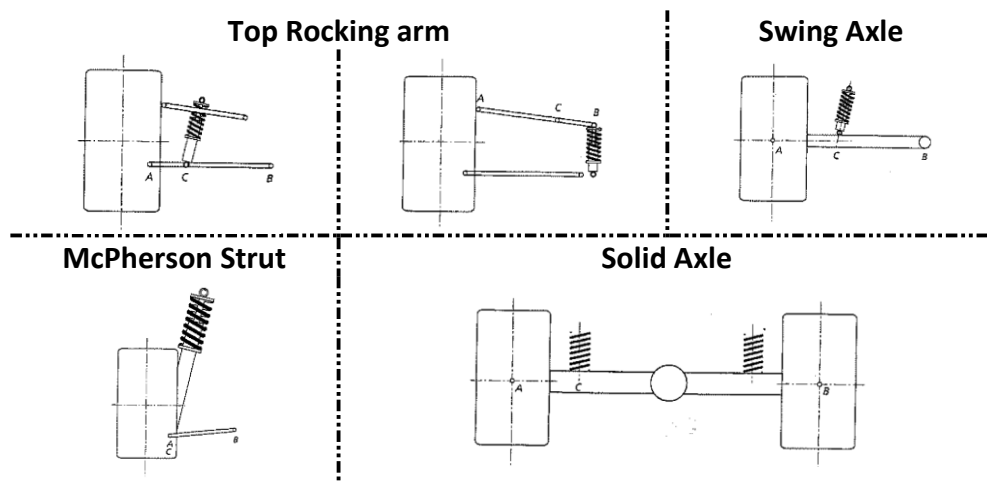


Figure 6 - Different suspension geometry (Baylos 2016)

The mechanical advantage has been defined mathematically in equation (2.10).

$$mechanical\ advantage = \frac{\overline{AB}}{\overline{BC}} \quad (2.1)$$

It can be seen and concluded that, for the McPherson system, the mechanical advantage is equal to 1, since the distance AB is numerically equal to the distance CB when this system is applied, regardless of its dimensions.

The lever effect is considered, in which the displacement of the wheel is transmitted to the compression of the spring, and the relationship between the two is designated the installation rate, IR. The inverse of the mechanical advantage was also considered, as shown in Figure 7.

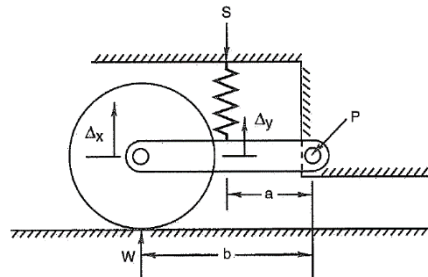


Figure 7 - Installation ratio (William F. Milliken 1995)

Therefore, by observing and analysing the illustration in Figure 7 the wheel and spring are connected to the suspension arm which rotates at point P at a distance of b and a from point P, respectively. A vertical displacement of the suspension arm rotating at pivot point P causes a variation  $\Delta x$ , as the wheel moves vertically, and  $\Delta y$ , the compression in the spring. The relationship between these two factors, the rate of change of the spring with the displacement of the wheel, defines the installation ratio.

### 2.3 Vehicle Dynamics

Vehicle dynamics is a specialised field of study and engineering that focuses on understanding and optimising the behaviour of vehicles. In this project, it focuses on motorsport, particularly rallies, although the following explanation is applicable to other racing series. It encompasses the complex interactions between a vehicle, the road, and the driver, with the purpose of obtaining the best possible performance, safety, and handling characteristics.

In racing vehicles, where speed, performance, and driving at the limit of what is possible, the suspension system plays a crucial role in controlling the vehicle's dynamics. It includes factors such as camber, toe, and caster angles, and is carefully adjusted to optimise tyre contact with the road and to control weight transfer during acceleration, braking and cornering. These vehicles are designed to behave optimally in high-speed, high-stress conditions, so it is important that the vehicle responds to the driver's commands and the engineers work to find a balance between stability and agility.

The weight distribution between the front and rear axles, as well as the side-to-side balance, are carefully managed to optimise cornering behaviour and overall stability, with the consideration of a critical component in dynamics vehicle, the tyre. Every engineer needs to take into account tyre compound, tyre pressure, and temperature management to maximise grip and traction.

In addition to vehicle dynamics considerations, other features such as driver input and feedback, and data acquisition play a vital role in vehicle dynamics. The driver provides information on the vehicle's behaviour and works closely with the engineers to fine-tune the setups according to their driving style and preferences. Real-time data collection during tests and races makes it possible to monitor the vehicle's performance, evaluate cornering speeds, and braking and acceleration distances.

Vehicle dynamics in motorsport is a highly specialised and constantly evolving field that combines engineering expertise, advanced technology, and the knowledge of racing drivers to push the boundaries of what is possible in the world of motorsports. It's a field in which even

the smallest adjustments can make a significant difference to the performance and competitive edge of a racing vehicle.

### 2.3.1 Sprung Mass and Unsprung Mass

When describing the distribution of a vehicle's mass and how this affects the vehicle's dynamics, in particular its suspension system, the term sprung, and unsprung mass is used.

The sprung mass refers to the part of a vehicle's total mass that is supported by the suspension system and moves in response to road irregularities. It includes the vehicle's main structure, which comprises the body, engine, transmission, and other components that are located above the suspension system. Changes in sprung mass distribution significantly affect the vehicle's handling and performance.

The unsprung mass refers to the part of a vehicle's total mass that is not supported by the suspension system and that interacts directly with the road surface. It is directly affected by road imperfections, bumps, which include components located close to the suspension system, such as wheels, tyres, brakes, and parts of the suspension itself. Optimising the distribution and minimising the unsprung mass is crucial in terms of responsiveness and surface grip.

Each of these masses has a centre of gravity which is a critical consideration in vehicle dynamics, which means the points where forces are applied that are equivalent to the forces to which the components are subjected, such as lateral forces and longitudinal forces when cornering, braking and acceleration.

To summarise, understanding the concepts of sprung mass and unsprung mass is essential to understanding the dynamics of a vehicle's suspension system, its performance, and its handling capabilities. Achieving an optimum balance between these two mass components is a fundamental aspect of vehicle design and suspension engineering.

## 2.4 Tyre Behaviour

Tyre behaviour is highly non-linear and dependent on the environment, making it a complex factor in vehicle dynamic. The interaction with the road will dictate the control and stabilisation of the vehicle, based on the traction, braking and cornering forces and torques developed. In addition, the tyre supports the weight of the vehicle and resists external road disturbances.

Despite its complexity, it is possible to define and isolate certain aspects of behaviour and, in the following topics, explain their characteristics separately.

### 2.4.1 Wheel Coordinate System

Figure 8 shows the coordinate system that is also important for the tyre. It involves two axes parallel to the local road plane,  $X_T$  and  $Y_T$ , with the  $Z_T$  axis normal to the local road plane and pointing positively upwards. The intersection of the wheel plane and the road plane defines the orientation of the  $X_T$  axis. This coordinate system has its origin at centre of the tyre's footprint, considering the tyre to be stationary.

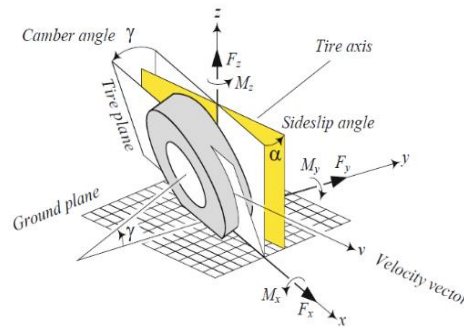


Figure 8 - Forces and moments (Rajamani 2005)

The angle  $\alpha$  is the slip angle. The angle  $\gamma$  represent the wheel camber. When considering the case of a steered wheel, angle  $\delta$ , the steering angle, will also be considered.

### 2.4.2 Tyre contact patch or Footprint

The area of the tyre tread in contact with the ground at any given moment is known as the footprint. The tyre's ability to withstand the forces and moments of the vehicle is related to the footprint, in order to maximise performance.

### 2.4.3 Grip

In the tyre's footprint, two surfaces come into contact and friction occurs. There is static friction and dynamic friction. Static friction is the force that needs to be applied for movement to begin, while dynamic friction, which has a lower value than static friction, is the force needed for relative movement to continue once it has begun. Interaction can be divided into two mechanisms, mechanical bonding, and chemical bonding.

Mechanical purchase accounts for a third of the maximum grip and is independent of the friction between the ground and the rubber, still operating at low grip. The chemical bond related to fresh rubber has a very strong adhesive force, which means the possibility of a much higher torque applied by the tyre, before it starts to slide. This increased grip has the disadvantage of rapid tyre wear, as the new rubber is progressively exposed, and a compromise is needed between maximum grip and tyre wear.

### 2.4.4 Tyre Pressure

The pressure of the tyre affects its behaviour in different ways, and the range of permitted pressures is usually defined by the tyre manufacturer. Lower or higher pressure in tyre will compromise performance, and the ideal pressure is defined to have a proportional share of the load, so that the centre will be supported mainly by the pressure and the sidewalls. The ideal inflation pressure is shown in Figure 9, on left-hand side.

With overinflation of the tyre, as seen in the centre of Figure 9, the central region is where only contact is made, which leads to overheating of the tyre, due to a reduced region through which the shear force passes for the entire tyre. It also has an effect on the tyre's spring rate, leading to a lower contribution from the tyre to the vehicle's vertical spring.

The right-hand side of Figure 9 shows an underinflated tyre, where the outer regions of the contact area carry most of the load due to the rigidity of the sidewall.

The best pressure is a compromise between the maximum grip obtained at lower pressures and the best performance obtained at higher pressures, which has only been found through experimentation and experience.

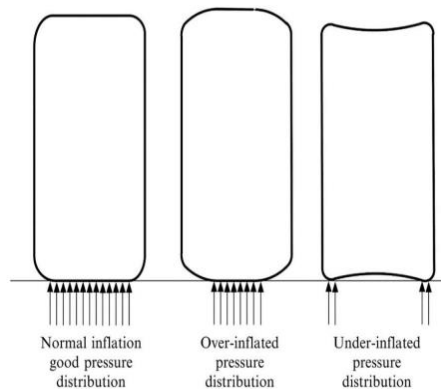


Figure 9 - Effect of tyre pressure on contact patch (Balkwill 2018d)

### 2.4.5 Temperature

As the temperature rises, the rubber becomes softer, which increases mechanical and chemical grip. However, the material properties of the tyre decrease, which means that the tyre fails under less load, resulting in lower performance.

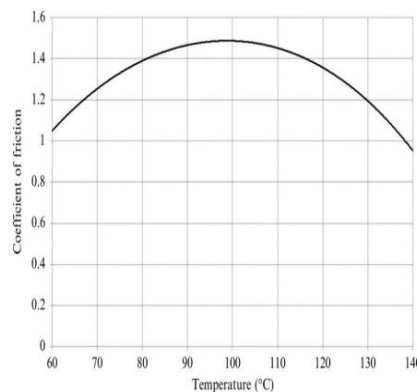


Figure 10 - Effect of temperature on grip (Balkwill 2018d)

Figure 10 shows the relationship between the coefficient of friction and temperature, where an increase in temperature results in better grip up to a certain point. At temperatures above 100-110°C, an increase in temperature will translate into a reduction in grip.

### 2.4.6 Tyre compound

The construction of modern tyres is complex and the result of years of development. Without going into detail about the internal construction, the area where material properties play a key role is in the rubber tread, which has direct contact with the ground. The best grip will be on a softer compound, reaching the functional temperature more quickly, but wear will be greater and the service life shorter, and vice versa for the hard compound.

### 2.4.7 Slip Angle

The term slip is related to a deviation from a certain ideal and is necessary for the transmission of forces by the tyre. The slip angle is relevant during lateral forces and is

geometrically characterised as the angle between the direction imposed by the steering wheel and that assumed by the tyre. Figure 11 illustrates the mechanism of the slip angle.

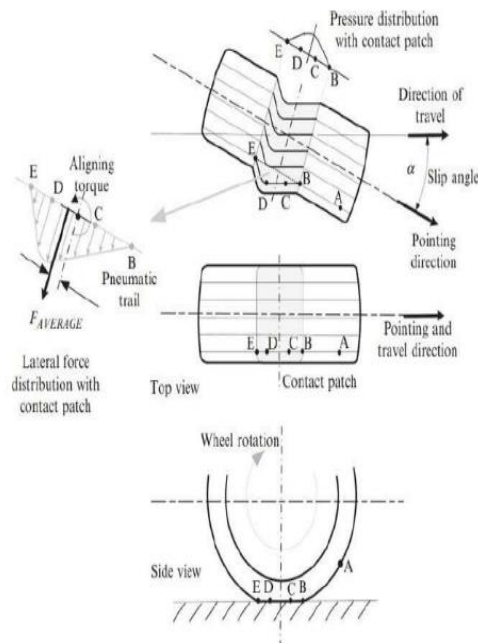


Figure 11 - Schematic of slip angle (Balkwill 2018d)

When a slip angle is generated, the footprint in contact with the ground and therefore subject to friction, resists the turning moment and tends to deform in contact with the ground and the side walls.

For a better understanding of the mechanism, let's look at the top representation in Figure 11, which shows the generation of lateral force, with the tyre directed and moving to the right. Following a rubber element over a surface, with position 'A' being the starting point, where the element is in the air and does not experience displacement forces from the ground. On the trajectory from 'A' to 'E', without the movement of the steering wheel, the element will follow the dotted trajectory shown and the behaviour is the same as in the middle representation. However, with the movement of the steering wheel, when the element encounters the ground 'B', it binds to it and the element has to move to point 'C'. From 'B' to 'C' it is observed that the element has been displaced laterally, in the direction of travel, creating an elastic force in that direction. During the movement from 'C' to 'D' two effects are present: the increase in lateral displacement and, from the vertical load, the flattening and spreading of the circular profile. The upper part of the representation of the tyre shows the pressure distribution in the contact patch.

Halfway along the contact patch, around point 'D', the vertical load begins to decrease, but the lateral displacement continues to increase. However, the force to restore the element's position is increasing, and the force between the element and the ground is tending to decrease. Shortly after 'D', the element reaches a point where the direction changes, and the element begins to return to the rest position. When it reaches position 'E', the element leaves the contact patch, and also throughout the process.

The left-hand side of Figure 11 shows the lateral force from the entrance of the element to its exit from the contact patch.

It is possible to see the generation of the aligning torque, the lateral force does not act on the centre line, and the distance from the contact patch to the lateral force is called pneumatic trail. This torque, which serves to pull the steered wheel into the straight-ahead position, will



have an impact on the feedback for the driver to know how much steering is applied to the tyre, so that drivers know the direction of the wheel without looking at the steering wheel.

From the above demonstration of the slip angle and lateral force generation, with the slip angle at zero no lateral force is generated. Necessarily, it can also be seen that if the tyre is generating lateral force, there must be a slip angle.

### 2.4.8 Lateral Force

The lateral force on the tyre is the component of the force normal to the intersection of the road plane and the wheel plane,  $F_y$  in Figure 12.

These forces are needed to control the vehicle's steering and it is considered a very important function of the tyre to accurately translate the driver's commands.

From topic 2.4.7, the dependence of lateral force on the slip angle is expected, with a null slip angle corresponding to a null lateral force, and it is also possible to consider an increase in the lateral force as the slip angle increases.

Figure 12 shows a graph of the slip angle versus lateral force, from Milliken & Milliken, where it is present for a given tyre, however the general shape remains independent, with the slip angle values varying for the maximum lateral force and the maximum lateral force corresponding to the tyre design. It is important to note that the graph shown corresponds to a vehicle weighing 816 kg, since the load on the tyre will have an impact on the shape, especially in the linear range.

By observation, it can be seen that the tyre works in three distinct phases: elastic or linear, transitional, and frictional, where the gradient in the elastic range is related to cornering stiffness. Cornering stiffness is defined as the necessary cornering force developed for each degree of slip angle generated. A higher cornering stiffness, a greater cornering force required to generate a degree of slip angle, results in a lower steering angle correction to maintain the intended trajectory.

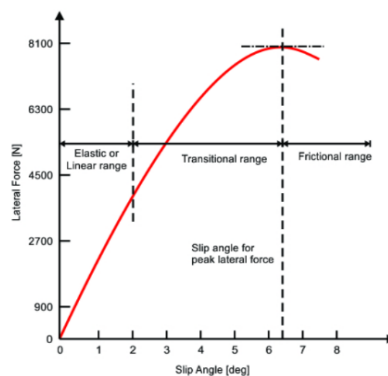


Figure 12 - Slip angle vs lateral force (William F. Milliken 1995)

In the transition phase, the increase in slip angle results in an increase in lateral force, but not a proportional one, which can be extended over a substantial range of slip angles, with advance warning of a loss of traction, or more abruptly, resulting in a sudden loss of traction.

Finally, in the friction phase, an increase in the slip angle corresponds to a decrease in the lateral force on the tyre.

Milliken & Milliken state that in dry conditions, racing tyres reach their peak lateral force at slip angles of around  $3^\circ$  -  $7^\circ$ , and that in wet conditions, the peak value will generally be lower, and that after the peak lateral force, the fall will be faster.

The ratio between the lateral force and the vertical load on the tyre represents the lateral force coefficient. This will lead to Figure 13, which shows, for different vertical loads, the variation of the lateral force coefficient with the values of the slip angle.

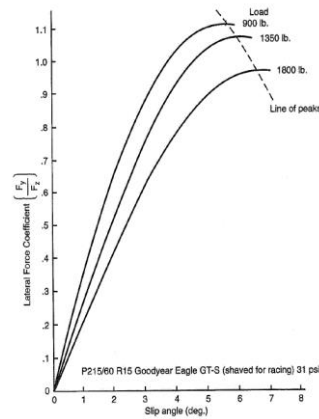


Figure 13 - Slip angle vs lateral force coefficient (William F. Milliken 1995)

The effect of the peak lateral force coefficient that is higher with lighter loads or lower with increasing load is designated the load sensitivity of the tyre, influencing the balance of the vehicle when operating close to the limit.

#### 2.4.9 Longitudinal Force

In the area where the tyre comes into contact with the ground, longitudinal forces must be developed in order to accelerate or brake the vehicle. The development of the longitudinal force can be seen in a similar way to the lateral force, with the existence of a region of elastic distortion and a region of sliding, although the slip angle is zero.

The braking force is described first, followed by the traction force, the reverse braking situation and ending with the slip ratio.

#### 2.4.10 Braking Force

To explain the generation of the braking force, a brush model is established, shown in Figure 14. As in the explanation of the slip angle at point 2.4.7, an element point on the surface will be followed from before it enters the contact patch until it leaves the contact patch. The starting point refers to point A on the tyre and point B on the road surface which represent point 'A' when it comes into contact with the ground. Points 'C' and 'D' refer to a line, designated as a line element which, being an elastic connection, allows a force to be applied between the two points and represents the deformation suffered. When an element comes into contact with the ground while braking, it has a forward velocity in relation to the ground, and from 'C' to 'E' there is a displacement in the x direction, as can be seen in Figure 14. A tension develops in the x direction in the brush element, which exerts a force in the rearward direction, braking the movement and decelerating the vehicle.

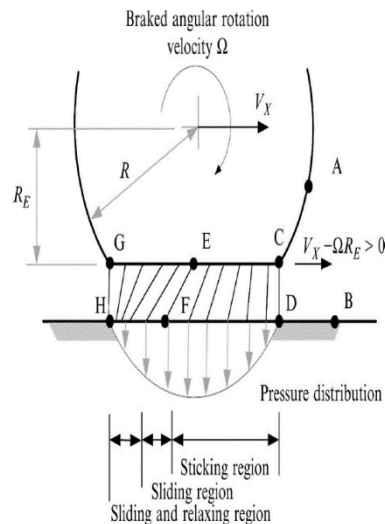


Figure 14 – Brush model for braking (Balkwill 2018d)

In relation to the different velocities between the points ‘C’ and ‘D’ can be translate as equation (2.2),

$$V_x - \Omega R_E \quad (2.2)$$

Where:

$V_x$  is the velocity

$\Omega$  is the braked angular rotation velocity

$R_E$  is the point E radius.

That, in the case of braking, this quantity is positive.

When the element reaches the end of the contact patch, the vertical load is zero and the brush element is vertical again, just as it was when it entered the contact patch.

For braking, and for the traction condition that will be present below, there are three regions within the contact patch. The sticking region, the first, where the elements of the tyre make good contact with the ground. The sliding region, the second region, in which the tension in the brush elements decreases due to the reduction in vertical load. Finally, the third region, the sliding and relaxing region as the tyre approaches the exit from the contact patch, in which there is complete relaxation, and the brush elements return to their vertical orientation.

#### 2.4.11 Tractive Condition

The tractive condition is the reverse of the situation analysed in point 2.4.10 for the braking condition. The brush elements will be inclined in the opposite direction and point ‘C’ will move to the left in relation to point ‘D’. In this condition, the forces on the brush elements will push the tyre forward and a traction force is developed. It should also be noted that the difference in velocities in the tractive condition is a negative quantity.

#### 2.4.12 Longitudinal Slip Ratio

Just as there is a lateral slip angle, there is a longitudinal equivalent designated the slip ratio. The slip ratio is the relationship between the forward velocity and the velocity of a point on the effective rolling radius, on the tyre surface.

It can be expressed as follows equation (2.10),

$$SR = \frac{\Omega R_E}{V} - 1, \alpha = 0 \tag{2.3}$$

Where it can be seen that for free rolling  $SR=0$ , for blocked braking  $SR=-1$  and for spinning it is  $SR=+1$ .

In Figure 16 and Figure 15, relating to traction and braking respectively, it can be observed that the forces are linear up to the normalised force with a maximum value of 1. After the maximum force peak, the forces begin to decrease, which is most noticeable in the traction curve, Figure 16. When the peak of the slip ratio is exceeded, there is also an unstable behaviour that tends towards blockage, in braking, and no force applied to the tyre, or spin-up, in traction, with the curve stagnating.

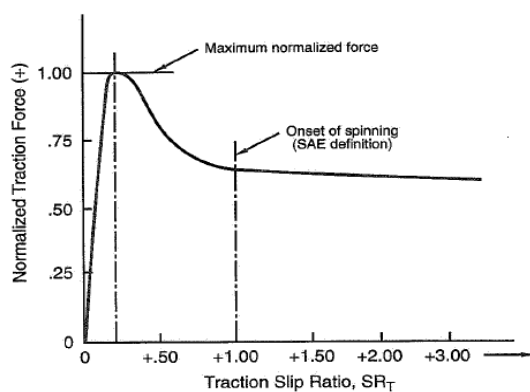


Figure 16 - Traction behavior curve, slip angle = 0° (William F. Milliken 1995)

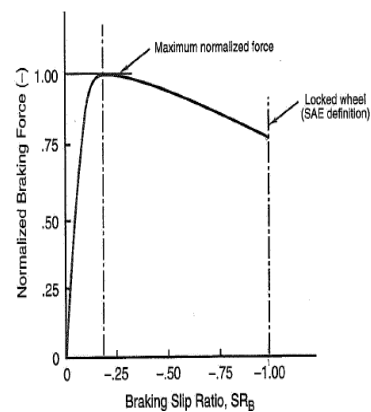


Figure 15 - Braking behavior curve, slip angle = 0° (William F. Milliken 1995)

### 2.4.13 Vertical Force

The vertical force supports the load on each corner of the vehicle and is also known as the normal force on the tyre. When the aim is to operate close to the limit, tyre load is particularly important, as it determines the force available for traction, braking and lateral force.

The following figures, Figure 17 and Figure 18, show how the vertical load affects the maximum lateral force that can be generated and the coefficient of friction, respectively. In Figure 18, it can be seen that the maximum lateral force against the vertical load is not linear,

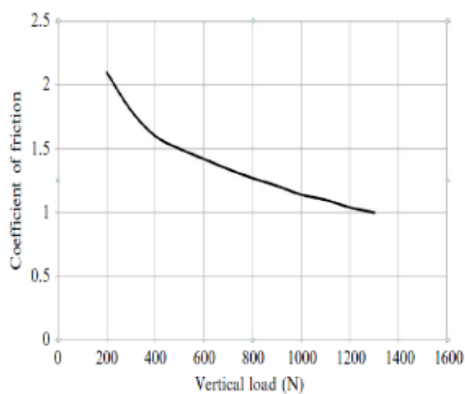


Figure 17 - Coefficient of friction vs vertical load (Balkwill 2018d)

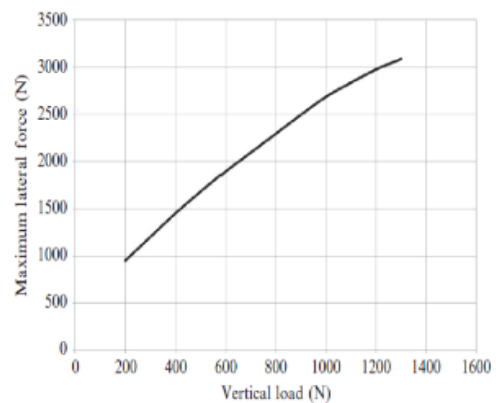


Figure 18 - Lateral force vs vertical load (Balkwill 2018d)

it is close but there is a small curve. Figure 17, shows that the lower the vertical load, the higher the coefficient of friction.

#### 2.4.14 Aligning Torque

The aligning torque,  $M_z$  in Figure 8 at point 2.4.1, is the moment about the vertical axis generated to counteract the steering angle so that the wheel returns to a straight position. It can also be seen in Figure 11 at point 2.4.7, where the average of all the element forces,  $F_{average}$ , is applied behind the centre line of the contact patch, which generates a torque, designated aligning torque.

This realignment of the wheel provides feedback to the driver, as they feel the amount of steering applied to the tyre.

#### 2.4.15 Rolling Resistance

The longitudinally moving tyre resists movement and is a concern in power calculations.

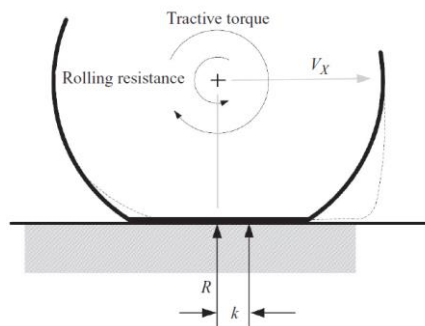


Figure 19 - Rolling resistance in tractive torque (Balkwill 2018d)

Consider a tyre in traction, Figure 19, where a traction torque is applied to the axle and the rotation is clockwise. With the brush model presented earlier and knowing that the centre line will move backwards in relation to the contact patch, the tyre will deform and take the shape of the dashed line. From this deformation, the vertical force,  $R$ , will be at distance  $k$  in front of the wheel axle, so the product  $Rk$  gives a moment that resists the traction torque, the rolling resistance.

If the braking condition is considered, the situation is reversed, and the torque applied is the opposite of the braking torque.

Also, considering the hysteresis display of tyre rubber, it follows that the force causing the distortion is not recovered when the force is relaxed. As a consequence, every moment of bending of the element, from compression and relaxation through the contact patch, will result in a loss of energy, causing rolling resistance.

This loss of energy will be one of the sources of internal heating and will increase the temperature of the tyre, which on the one side is advantageous for increasing the coefficient of friction, but the increase in grip will reduce the life of the tyre.

#### 2.4.16 Friction Circle and Ellipse

Above the lateral force was analysed as a result of the slip angle, the longitudinal force as a result of the longitudinal slip, however the forces generated by the tyre do not act separately, but the tyre experiences both conditions together.

In this section, the lateral and longitudinal forces are combined, developing a single diagram made up of friction circles and ellipses.

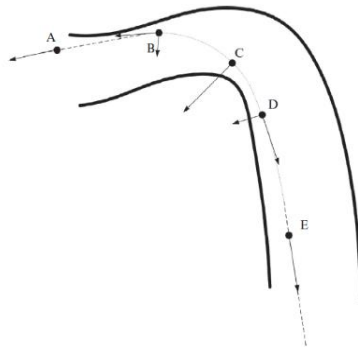


Figure 20 - Tyres forces through one corner (Balkwill 2018b)

Looking at Figure 20, it is possible to see the forces acting on the tyre along a corner. At point 'A' the car is approaching the corner, the driver applies the brakes with the straight steering, as a result only longitudinal force is generated and there is no lateral force development. Shortly after point 'B', the driver applies the steering and begins to lift his foot off the brake pedal in the 'turn-in', reducing the longitudinal force still significantly and developing a modest lateral force. Point 'C' represents the apex of the corner, the driver does not apply the brakes or the accelerator, there is no longitudinal force, only lateral force with all the tyre's capacity to generate this force. At the exit of the corner, point 'D', the driver starts to apply the accelerator, as a result of which longitudinal force is generated and lateral force is reduced. At point 'E' the corner is finished, only the accelerator is applied, as a result only longitudinal force is developed.

This whole process is repeated in the following corners.

By drawing a diagram and plotting the combined lateral and longitudinal forces, a representation similar to Figure 21 is obtain, which corresponds to the corner explained above.

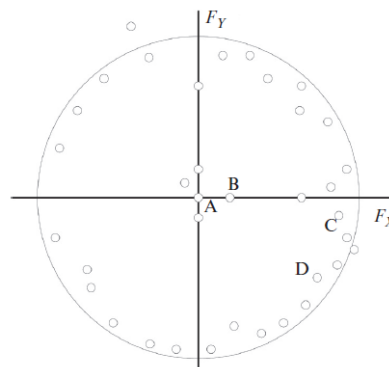


Figure 21 - Friction circle (Balkwill 2018b)

With  $F_x$  representing the lateral force and  $F_y$  the longitudinal force, positive  $F_y$  is the traction force and negative  $F_y$  is the braking force. The interest in representing the combined forces lies in the fact that the limit is the maximum force that the tyre can generate under these conditions. This represents the limit at or near which the driver must be able to drive in order to obtain the tyre's maximum capacity.

For some tyres, the diagram is not a perfect circle, as in Figure 21, but can be slightly elliptical in the outer envelope.

## 2.5 Wheel Alignment

Wheel alignment, also known as tyre alignment, is a crucial maintenance procedure to ensure that a vehicle's wheels are correctly aligned with each other and with the vehicle's geometry.

In the context of vehicle dynamics racing, wheel alignment is a critical aspect of optimising a racing car's performance. Obtaining precise and carefully tuned wheel alignment settings can have a significant impact on the handling, grip, and overall speed of a racing vehicle. In terms of alignment type and wheel settings, camber angle, caster angle and toe angle are considered, which allow for precision and consistency, tyre temperature management and driver feedback.

In the dynamics of racing vehicles, every small adjustment in wheel alignment can make a substantial difference to performance. Analysing the data and researching the ideal alignment is part of the process of continuous improvement that enables racing vehicles to push the boundaries of performance.

### 2.5.1 Camber

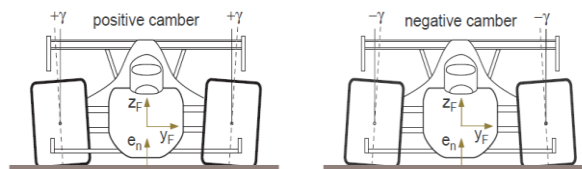


Figure 22 - Positive and negative camber, respectively  
(vehicle dynamics, 2006)

Camber is defined as the angle of the wheel in relation to an imaginary vertical line that passes through the centre of the wheel when looking at the front of the vehicle, as illustrated in Figure 22, and is denoted by the symbol  $\gamma$ . This angle can be positive, as on the left-hand side of Figure 22, where the top of the wheel tilts outwards, or, conversely, if the top of the wheel tilts inwards, the camber is said to be in negative, as on the right-hand side, or even zero.

In racing vehicles, negative camber angles are typically used, with the possibility of using different angles on all four wheels depending on the type of race or even circuit, in order to obtain maximum performance from the tyre. When the vehicle is cornering, the outer wheel will have more load due to weight transfer, but also, for the geometry of the suspension, the wheel will tend towards zero camber, resulting in a greater contact patch. If the static angle of camber is zero, it will tend to be positive and if it is positive, it will increase, resulting in tyre inefficiency.

The camber values must be well studied and determined for each case, as is the case in many aspects of engineering. An example of determining the ideal angle of camber in relation to tyre wear is measuring the temperature of the tyre at three points, the inner, middle, and outer section, Figure 23, at the end of the training or test session, where the temperature should be the most uniform between the three points.

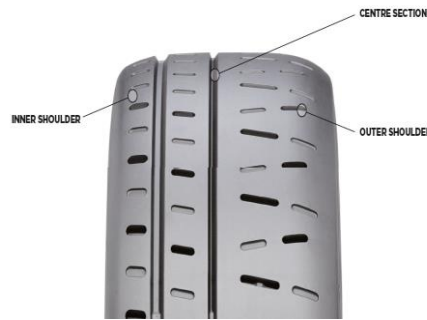


Figure 23 - Temperature measurement points on a tarmac tyre (Michelin 2001)

If the internal temperature is too high in relation to the others, the camber angle should be reduced, also avoiding excessive tyre wear in the internal section, Figure 24. Thus, analysing this parameter, tyre temperature, is an asset for improving the setup and the possibility of uniform tyre wear.

It's important to note that the tyre's operating temperature depends on the compound, the harder the compound the higher operating temperature, and the more energy the driver needs to put into the tyre to bring it up to the ideal temperature.

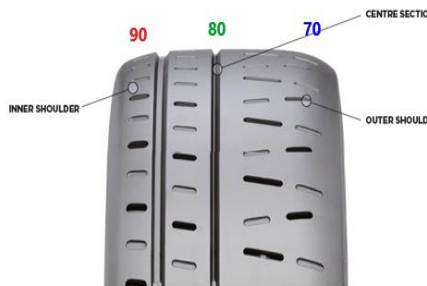


Figure 24 - Example of too much camber on tarmac tyre (Michelin 2001)

### 2.5.2 Camber Thrust

The camber thrust is considered a second source of lateral force. Considering Figure 25, an element that in equilibrium position is in "A" but is forced to be in position "B", on the right side of the figure, results in a vertical load that supports the load of the vehicle and a horizontal force with the same direction as the inclination of the tyre, present on the left side. This horizontal force that appears is the camber thrust, and the camber thrust is dependent on the camber value.

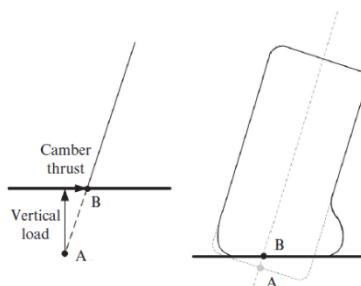


Figure 25 - Camber thrust (Balkwill 2018d)



### 2.5.3 Caster Angle

The caster angle is defined as the inclination of the steering axis in relation to the vertical, Figure 26. It can be seen in Figure 26 that the intersecting point on the ground of the steering axis is ahead of the centre point, which illustrates a positive caster angle, which is the backward inclination of the steering axis.

When the wheel is steered to the right or left, the centre of friction between the tyre and the ground moves laterally, creating a rolling radius, which results in a rolling moment that brings the wheel back to a straight line. In general terms, a positive caster angle gives the vehicle the tendency to travel in a straight line, or to return to it when deviating from it.

In an extreme case, if the positive caster angle is too high, it will contribute to the steering quickly returning to a straight line and making cornering extremely difficult.

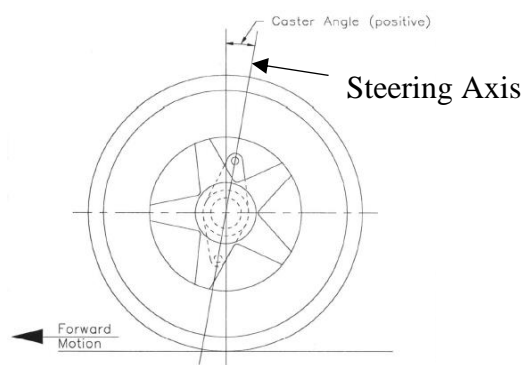


Figure 26 - Caster angle (Crahan 2023)

### 2.5.4 Ackermann Steering Geometry

Observing the vehicle on a bend, it can be noticed that the inside wheel has a smaller cornering radius than the outside wheel, which is more pronounced when the vehicle is wider, and the corner is steeper.

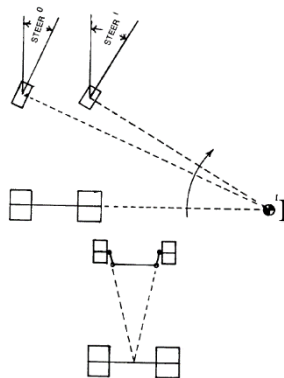


Figure 27 - Ackermann steering geometry principle (Smith 1978)

Figure 27 illustrates the basic concept created to resolve the fact of the different radiuses on each wheel, in which the inner wheel will have a greater steering angle than the outer wheel, and if an extended axis of steering arms is created, the point of intersection is in the middle of the rear axle. The point of intersection on the line with the rear axle, designated as the instantaneous centre of turn I in Figure 27, is the centre of the concentric circles on the wheels that will be tangent to each other.

Figure 28 shows different steering geometries, in the middle the classic Ackermann used from an early age, on the right the currently common parallel steering and in competition vehicle the Reverse Ackermann geometry is common, according to Milliken & Milliken.

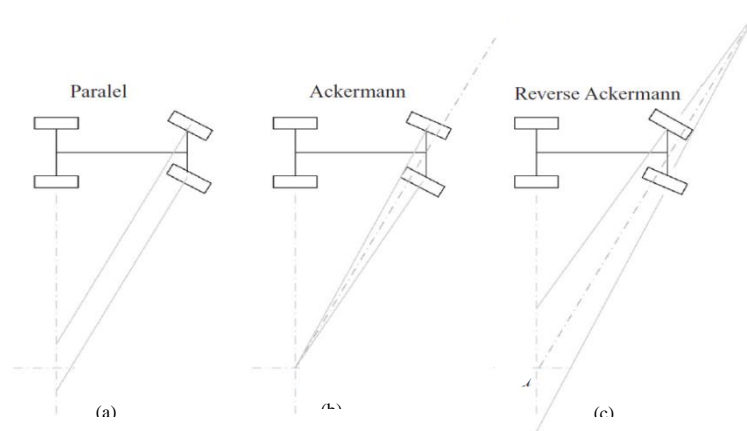


Figure 28 - Different steering geometry (a) parallel, (b) ackermann and (c) reverse ackermann (Balkwill 2018b)

“...the authors feel that parallel steer or a bit of reverse Ackermann is a reasonable compromise. With parallel steer, the car will be somewhat difficult to push through the pits because the front wheels will be fighting each other. At racing speeds, on large radius turns, the front wheels are steered very little, thus any Ackermann effects will not have a large effect on the individual wheel slip angles, relative to a reference steer angle, measured at the centerline of the car.” (William F. Milliken 1995)

### 2.5.5 Toe

The toe is not only a parameter that has an influence on dynamic behaviour, such as a dynamically stable condition at toe-in, but it is also a parameter for the proper functioning of the tyre.

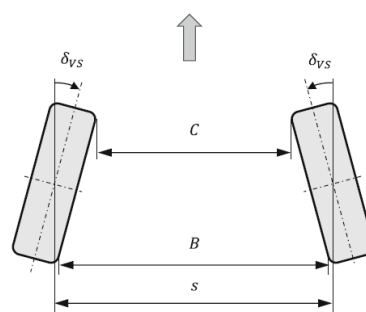


Figure 29 - Definition of toe (Guiggiani 2018)

To understand the definition of Toe, consider Figure 29. The difference between distances B and C describes the Toe. If measurement C is less than measurement B, the wheels point forwards, characterising the toe-in. If, on the other hand, measurement B is less than measurement C, then the wheel is pointing outwards, which describes the toe-out.

In a similar way to camber, toe can be beneficial to the vehicle’s performance or, if incorrectly set, it can be very detrimental to performance and also to the tyre. In extreme cases, when too much toe-in or toe-out is used, rolling resistance is increased, which translates into overheating of the tyre, leading to increased wear and potentially puncturing the tyre.

When the toe is well established it can improve performance, for example with rear toe-out it improves turn-in, when the vehicle turns, and weight transfer occurs to the outside wheel it will have an effect on oversteer during turning.

## 2.6 Centre of Gravity, CG

The location of the centre of gravity is crucial in any analysis of the vehicle's dynamic behaviour and is a fundamental determinant of performance, as well as being the point at which the entire weight of the vehicle can be taken into account, Figure 30. The reason is that the tyre's cornering force capacity depends on the wheel loads, since during cornering there is a distribution of weight transfer, which means that the wheel loads are not constant. In addition, the location of the centre of gravity is affected by changes in setup, such as varying the height of the vehicle or preparing the vehicle for gravel or asphalt, where the arm points on the subframes are different. Having the height of the centre of gravity in relation to the ground as low as possible provides better stability, reducing the tendency to roll, better cornering stability and the magnitude of the weight transfer.

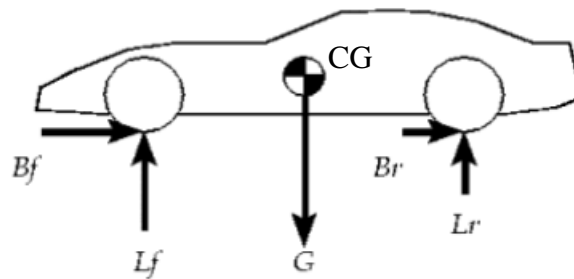


Figure 30 - Centre of gravity (Beckam 1991)

## 2.7 Instantaneous Centre

The instantaneous refers to a particular position of the linkage, and the centre refers to a projected imaginary point that corresponds to the point of the linkage's articulation at that instant. Representing the centre of a circle where the suspension of a wheel rotates at a specific location throughout the movement.

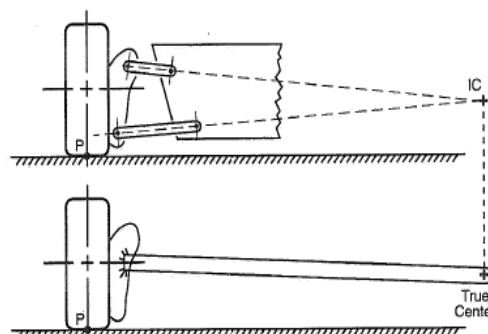


Figure 31 - Representation of Instantaneous Centre (William F. Milliken 1995)

In Figure 31 there is a suggestion in which two short links can be substituted for a longer one, with the suspension travel achieving the same rotation. The upper part of the Figure 31 shows that the location where the extensions of both arms intersect, in frontal or longitudinal view, is a virtual point, the Instantaneous Centre.

Slice the wheel in the vertical plane parallel to the vehicle's centreline, representing the instantaneous centre in the side view (along the y-axis). The connection of the two instantaneous centres gives rise to the instantaneous axis, around which the stub axle will move.

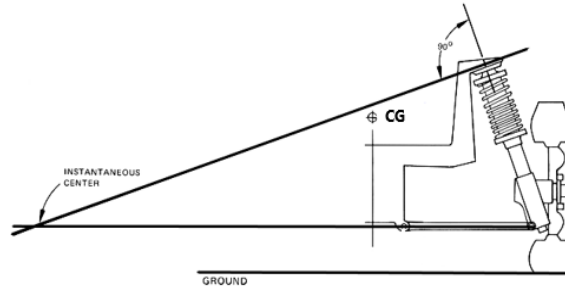


Figure 32 - Instantaneous centre in MacPherson suspension, front view (Rio 2009)

The instantaneous centre in the front view will define the camber variation rate, scrub motion, and part of the roll centre. In the side view, it will define the pitch behaviour and the caster change ratio.

When considering the MacPherson suspension, the instantaneous centre is shown in Figure 32. The centre is defined at the intersection between lower arm extension and a 90° line at the upper mounting point of the suspension structure.

Similarly, the instantaneous centre is determined in the side view, as seen in Figure 33. With these two points, the instantaneous axis is established.

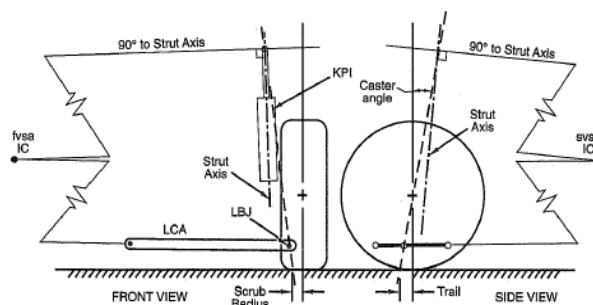


Figure 33 - Instantaneous centre MacPherson in front (left side) and side view (right side) (William F. Milliken 1995)

## 2.8 Roll Centre

The roll centre of a suspension is a theoretical point around which the body will rotate instantaneously, with the front and rear suspensions having different roll centres. It can be considered the most powerful adjustment in suspension analysis, as it has an immediate effect on the vehicle's handling.

Can be found by projecting a line from the centre of the tyre's contact patch, (note that this does not represent the middle of the tyre because the tyre can have slope, camber, and the tyre is not parallel to the ground) to the instantaneous centre in the front view. The intersection of the line on each side gives us the roll centre of the sprung mass, presented in Figure 34.

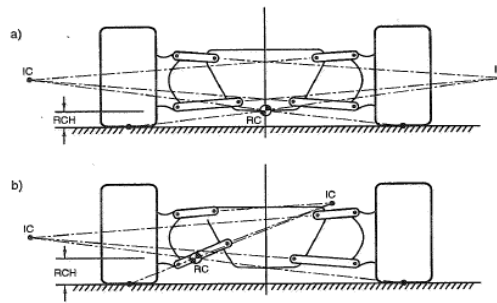


Figure 34 - Representation of roll centre in symmetric (a) and asymmetric (b) suspension geometry (William F. Milliken 1995)

From Figure 34 (b) it can be seen that the roll centre is not necessarily on the central line of the vehicle, in asymmetric suspension geometry or when the vehicle assumes a roll angle in a corner.

A higher roll centre results in a smaller rolling moment around the roll centre but considering that the lateral force of the tyre generates a moment around the instantaneous centre that pushes the wheel down and lifts the sprung mass, this is known as jacking.

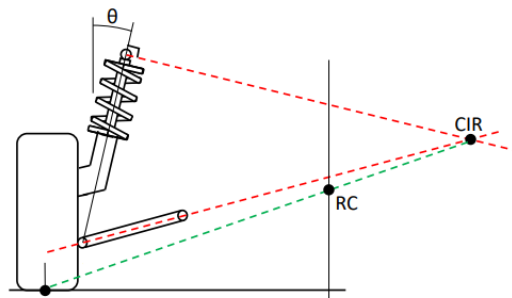


Figure 35 - Roll centre (RC) in MacPherson suspension (Ferreira 2023)

Figure 35 shows the roll centre in MacPherson strut suspension, where a line is drawn between the instantaneous centre and the tyre's contact patch, and considering the symmetry in the suspension geometry, defining the roll centre.

## 2.9 Anti-Dive

In the situation of braking, weight is transferred from the rear axle to the front axle, which contributes to an increase in the load on the front axle. The increased load causes a greater compression effect on the suspension.

Anti-dive means the design of the front axle to prevent the front from lowering under braking.

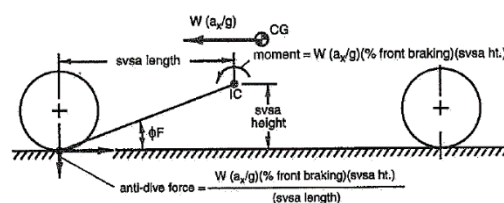


Figure 36 - Anti-Dive free body (William F. Milliken 1995)

The free body anti-diving diagram is illustrated in Figure 36, which can be found in Milliken & Milliken and is defined by the equation (2.10).

$$\text{Anti - Dive front (\%)} = \frac{\zeta \times l \times \tan A}{h} \quad (2.4)$$

Where:

$\zeta$ , is % front braking

$l$ , is wheelbase

$A$ , is angle between the ground and the virtual line from the tire contact point until the IC

$h$ , is CG height.

From equation (2.4), the percentage of anti-dive at front depends on the height of the centre gravity, as well as the distance between the front axle and the instantaneous centre and the percentage of front braking, but at the same time these parameters are constant.

It can be concluded that the anti-dive is directly dependent on the instant of rotation of the centre. Figure 36 shows that varying location of the IC, results in a variation in the angle  $A$ , and according to equation (2.4), the higher the  $A$  values, higher the anti-dive percentage, or vice-versa. Two extreme points can be defined, 100% and 0% anti-dive. The point typically referred to as 100% means that, during a braking application in which the weight is transferred to the front axle, the work done by the vehicle's damping is null, in other words, the entire load is sustained by the suspension arms. Thus, the anti-dive effect varies mainly with the geometry of the suspension arms, as these will be responsible for supporting all the weight transfer during braking.

However, from a dynamic point of view, this parameter is interesting for a better understanding of the vehicle's dynamics, and it is also clear that it is intrinsic to each vehicle. This doesn't mean that it isn't possible to mitigate the dive effect, there are means available, such as, adjusting the rebound of the damper (rebound, which will be explained later). This will increase the hydraulic inertia during the compression/decompression movement of the damper, and thus help to smooth out the weight transfer that take place over the front axle. Another example is the variation in the vehicle's ground clearance, which influences the location of its centre of gravity, and therefore the corresponding anti-dive effect.

## 2.10 Anti-Squat

In an acceleration situation, a similar logic can be applied to the rear of the vehicle. The rear of the vehicle has the same tendency when accelerating, as was seen when braking was applied by lowering the front, a fact dependent on the amount of anti-dive.

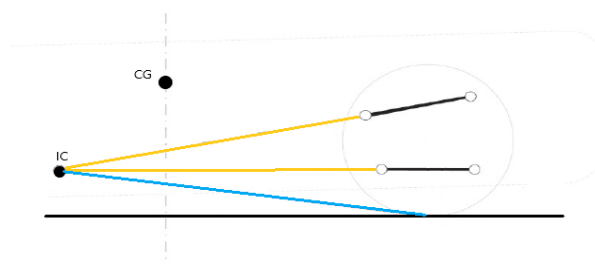


Figure 37 - Anti-Squat geometry

For this purpose, the anti-squat principle is identical to the anti-dive principle, although with the difference that it is relative to the movement at the rear. With a similar analysis on the rear suspension arms, Figure 37, the virtual line joining the point of contact of the rear tyre with the instantaneous centre of rotation associated with the rear arms of the wheel under analysis, it is possible to determine the height of the instantaneous centre on the line projected through the centre of gravity.

According to Carroll Smith, in his book *Tune to Win*, the lower limit of anti-squat is around 20% so that the rear tyres are not damaged by the effect. Because in practice, racing vehicles tend to generate some anti-squat, where the power-to-height ratio is higher than in ordinary vehicles.

## 2.11 Springs

In vehicles, coil springs or leaf springs can be found, but the subject of this work, which is related to racing vehicles, will only deal with coil springs, which have a constant diameter and are used in compression.

Figure 38 shows the nomenclature for the spring (a), and the typical ends used in (b).

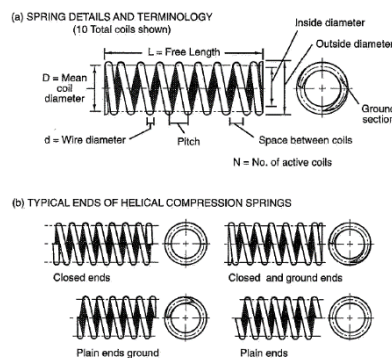


Figure 38 - Helical coil springs (William F. Milliken 1995)

Springs are defined by their stiffness, which is mathematically responsible for indicating the force per unit displacement. Thus, the force associated with the spring is given by the product of the spring stiffness  $k$ , and the displacement  $\Delta l$ , equation (2.5).

$$F_k = k \times \Delta l \quad (2.5)$$

For the case study, the suspension geometry, explained in point 2.2, refers to the suspension geometry referred to as MacPherson, which numerically means that the stiffness of the suspension is equal to the stiffness of the spring, which in fact makes it easier to understand the vehicle's damping behaviour.

Table 15 and Table 16 in Annexe 1 show the springs available and homologated by the FIA for the Skoda Fabia R5 EVO. In general, springs are distinguished by their stiffness value, as shown in Table 15 and Table 16.

In practice, the stiffness of some coil springs was tested with a digital coil spring tester, Figure 39. Since coil spring stiffness testers are valuable tools for guaranteeing the quality and performance of coil springs.



Figure 39 - Digital coil spring tester from Intercomp ("Intercomp")

For this practical measurement of coil spring stiffness, coils of 17,5 N/mm, 20 N/mm and 25 N/mm were selected. The measurements were repeated 3 times and the average values recorded and annotated, as shown in Table 1.

Table 1 – Registered coil spring stiffness values

17,5		20		25	
d [mm]	F [N]	d [mm]	F [N]	d [mm]	F [N]
0	0	0	0	0	0
10	17,5	10	20	10,01	25,5
20,01	33,5	20,01	40,5	20,04	51
30,02	52,5	30,02	61,5	30,02	77,5
40,02	69,5	40,01	82	40	104
50,01	87	50	103	50	130
60,02	104	60	123,5	60	156
70,04	121,5	70,01	144	70	182

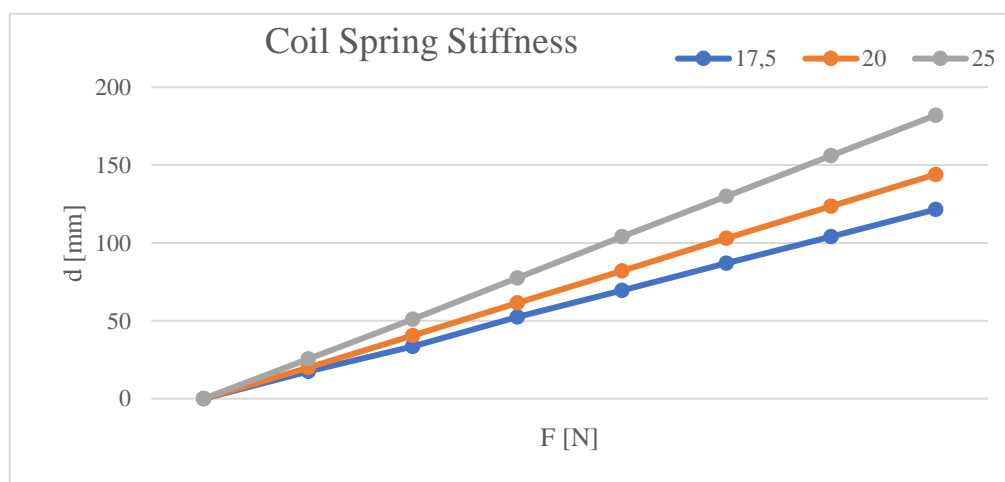


Figure 40 - Coil Spring Stiffness graphs of the recorded values

Figure 40 shows the graphs corresponding to the values in Table 1. It can be seen from the observation that there is a linear behaviour, as expected in this type of coil springs. This test was also carried out to check the stiffness of the coil spring to see if it begins to lose stiffness due to constant use, although this does not happen in these cases.



## 2.12 Dampers

“Sometimes I think that I would have enjoyed racing more in the days of the friction shock. Since you couldn’t do anything much to them or with them I would have spent a lot less time being confused” (Smith 1978)

Dampers must control the movement of the unsprung mass and suppress oscillation due to longitudinal and lateral acceleration. Unlike springs, which generate force with displacement, dampers generate force with speed. Given their unique properties, they control the rate of weight transfer from the springs and anti-roll bar.

The spring is compressed, influenced by the vertical acceleration, resulting in a large amount of kinetic energy stored in the spring. With the disappearance of the force that caused the spring to compress, the spring will extend with great force, pushing the wheel to full droop, moving to the driving height position. Without the damper, the spring oscillates at the natural frequency of the unsprung mass until all the stored energy has been dissipated. For this reason, the damper has the function of converting kinetic energy into thermal energy, which is dissipated into the air.

Figure 41 shows the damper assembly on the Skoda Fabia R5.

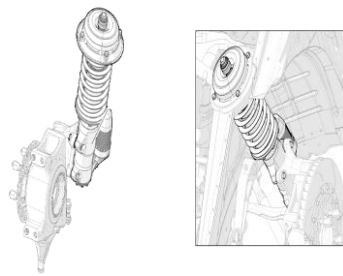


Figure 41 - Damper assembly on Skoda Fabia R5 (Skoda\_Motorsport 2023b)

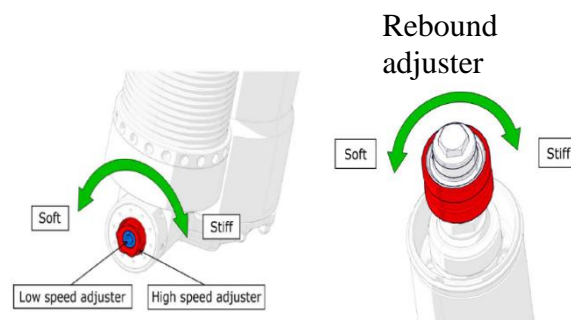


Figure 42 - Damper setting (Skoda\_Motorsport 2023b)

Figure 42 displays the possibility of 3-way, bump and rebound adjustment independently, with the compression adjusted for low and high speed separately. The compression adjustment is located at the bottom of the damper, in the remote reservoir, and the rebound adjustment is located at the top of the damper.

Describing the behaviour of the possible adjustable damper at low speed in compression for the more technical areas of the road, where vehicle speed tends to be lower. On the other side, high-speed compression is more effective on fast sections, due to the level of demand at the beginning of the damper’s movement. Rebound is responsible for hydraulic recovery, in

other words, how the damper extends after compression and the level of traction when braking and/or accelerating into corners.

Figure 43, shows the damper force versus displacement curve as a graphical representation of the relationship between the damping force generated by a damper and the displacement of the damper piston. The x-axis represents the displacement, and the y-axis represents the damping force generated by the damper at each corresponding displacement. The positive value on y-axis corresponds to the bump phase, when the damper is being compressed, while the negative value represents the rebound phase, when the damper piston is extending.

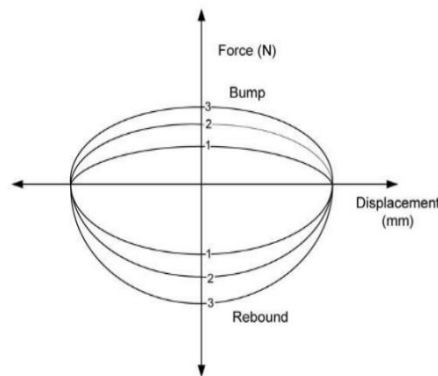


Figure 43 - Damper force vs displacement curve (Seward 2014)

The damper force vs displacement curve is a valuable tool for understanding and optimising the suspension system, in this case the damper, providing information on how a damper behaves in different conditions. This helps to achieve the desired balance between ride comfort and handling performance.

The relationship between damper behaviour and cornering behaviour will focus on Figure 44 and describe the different cornering phases.

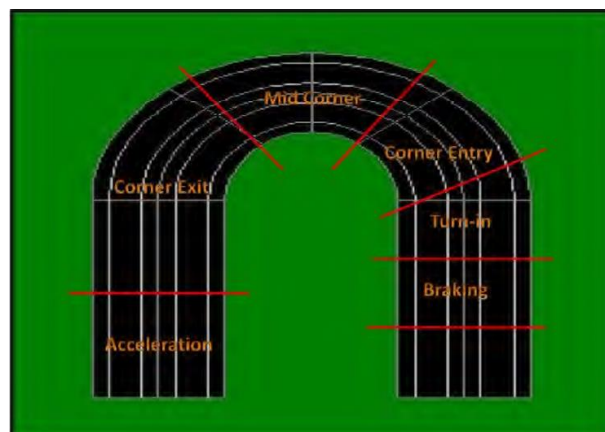


Figure 44 - Handling corner sections (Kasprzak 2012)

The first section is the braking zone, where the dampers control the transfer of weight from the rear wheels to the front wheels. With too little front compression, weight transfer occurs too quickly, loading the front wheels to a point where the tyres are unable to absorb the load, resulting in a loss of grip. On the other hand, if there is too much front compression, the weight transfer will occur too slowly, resulting in non-optimal braking, which will translate into the driver being delayed in making the turn.

If the rebound is too much at the rear, the weight transfer is like too much compression at the front and can make the vehicle unstable during braking, because it tends to lift the rear tyres

off the ground, losing grip. On the opposite side, if there is too little rebound (open rebound), the rear will bounce with the weight transfer to the front.

At the entrance to the turn-in section, most of the braking should be done and the downshift should be completed. This is when the driver makes his input to the steering and expects a response without hesitation.

In this area, the damper is used as a dynamic spring, as it only requires speed, while the springs require displacement, so it is possible to quickly load the outer wheel when the vehicle starts to roll. As a result, the vehicle will have good cornering response.

If the damping is too high, overloads the tyre, resulting in understeer. If it's too small, the vehicle becomes sluggish when turning. The stiffness of the anti-roll bar and springs must be considered.

On corner entry, weight transfer continues from the rear to the front and to the outer wheels. By using compression to control weight transfer, if a higher rate of weight transfer is required, less compression is used, otherwise, to slow down the rate, more compression is used.

If the compression isn't enough and the tyre starts to lose grip and even more control is needed, it is necessary to add rebound.

In the middle of the corner, the vehicle is in a stationary state, equilibrium is reached, and the front and rear rolling stiffness will be the basis of the corner. The dampers do not affect the handling at this phase.

At the exit of the corner is where the transition from turning to acceleration takes place. The process is the reverse of turn-in and braking, the weight transfer is from the front to the rear, in particular from the inside front wheel to the outside rear wheel. Controlling the rate of weight transfer is similar to corner entry and braking but taking into account the rear dampers.

In the acceleration section, the process is completely the reverse of braking, with the rate of weight transfer from the front wheels to the rear wheels having to be controlled.

It should be noted that the dampers are considered the fine tuning in the car. First, it's necessary to set the correct springs, the anti-roll bar for the steady part of the corner and then consider changing the damper setup for the weight transitions.

## 2.13 Vibration System and Damper

The last section introduced the damper, which is a typical mechanism in a conventional vibration system. It is responsible for dissipating kinetic energy by converting it into thermal energy, heating the viscous fluid and the surrounding air.

Figure 45 shows three curves, the underdamped curve in blue, the critically damped curve in green and the overdamped curve in red. Analysing the three curves, it is possible to confirm

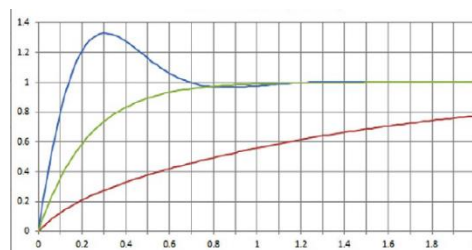


Figure 45 - Underdamped (blue), critically damped (green) and overdamped (red) analysis for response to step steer (Balkwill 2018c)

that for a step input, the curve with the best result is the critically damped one, resulting in quick stabilisation to the zero point on the damper. Compared to the other two curves, the overdamped

one has a long stabilisation time and the underdamped one has an overshoot, which is not a desirable response to a step input.

For the dynamic behaviour of a racing vehicle, it is of great interest that it is as stable as possible and that, under perfect conditions, the sprung mass does not exhibit any movement that disturbs driving. In this sense, it is important that the damper recovers as quickly as possible, without oscillation, to the imposed request.

Therefore, in order for the system to respond with the least sinusoidal behaviour and to settle as quickly as possible from the imposed request, it is necessary to impose a critically damped system, where the ratio of the damping coefficient  $c$  to the critical damping coefficient  $c_{cr}$  is designated as the damping ratio  $\xi$ , equation (2.10).

$$\xi = \frac{c}{c_{cr}} \tag{2.6}$$

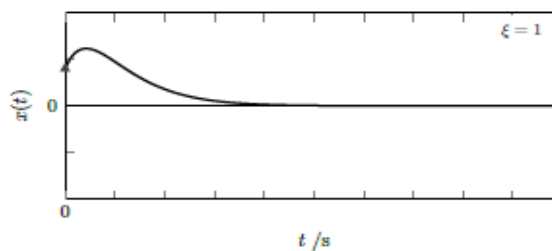


Figure 46 - System response to critical damping (Rodrigues 2021)

Where  $\xi = 1$  represents the critical damping, the vehicle has no resonance, Figure 46.

To corroborate the above and demonstrate objectively, in a competition damper, settling as quickly as possible in the response to the zero point, it was essential to use a critical damping system, consult Figure 47.

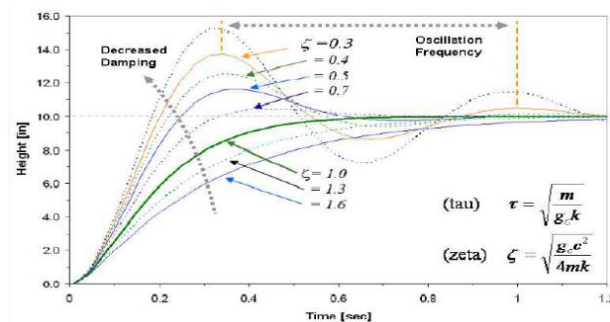


Figure 47 - Spring mass damper system response (Catto 2012)

Referring to Figure 47, it can be concluded that the critical damping with  $\xi = 1$  is the one that responds most quickly to the settling of the damper at the zero point, and deviating from this value will affect the response time with a decrease in damping at lower values of  $\xi$ .

Considering the damping coefficient numerically equal to the critical damping coefficient, expressed mathematically in equation (2.7).

$$c_c = 2 \cdot \sqrt{k_s \cdot m} \tag{2.7}$$

Where:

- $k_s$  is the spring rate,
- $m$  being the sprung mass.

The force can then be calculated in the same way using equation (2.10).

$$F_c = C \times \Delta \dot{Z} \tag{2.8}$$

The damping coefficient  $C$ , related before numerically to the critical damping coefficient, is dependent on the vertical displacement velocity  $\Delta \dot{Z}$ , to which the damper is subjected in ground irregularities. In practice, the vertical displacement can be determined using an extensometer.

Taking into account the vehicle's behaviour, the damper has the function of controlling the transmissibility of the unsprung mass which has an adverse effect on the vehicle's handling. Considering Figure 48, a simplified model for analysing only one of the four corners of the vehicle responsible for damping and the transmissibility of the unsprung mass, listed in Milliken & Milliken, 1995. In the graph shown, it is important to note that the stiffness of the tyre  $K_T$  is taken into account, which has a behaviour similar to that of a spring.

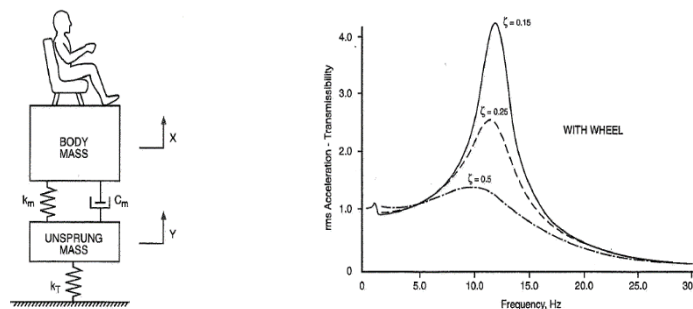


Figure 48 - One corner of the vehicle (right) and the transmissibility of unsprung mass (left) (William F. Milliken 1995)

Milliken & Milliken also state that a transmissibility value of 2,5 is a top value where above handling will be negatively affected and significant wheel hop will occur. Observing the graph in Figure 48, the transmissibility value – defined as the ratio between the vertical movement of the wheel and the amplitude of the road wave – is reduced as the damping value  $\xi$  increases. In relation to the critical damping shown above, with the damping value being optimal, the transmissibility will be greatly reduced.

Analysing the effect that damping has on handling behaviour, mentioned above, Figure 49 illustrates the effect of damping with lateral force and steering activity in opposite ground conditions.

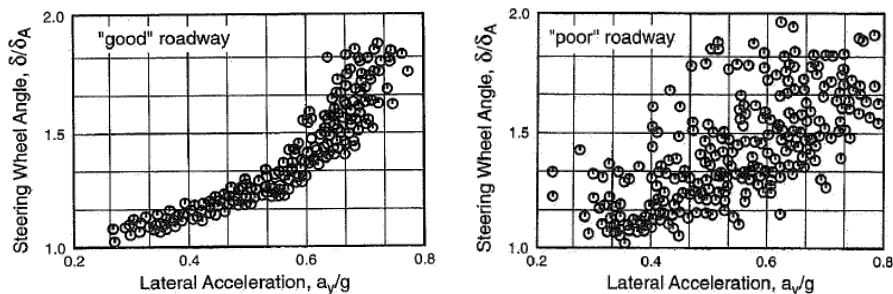


Figure 49 - Damping on curve for good and poor roadway (William F. Milliken 1995)

## 2.14 Anti-roll bar

The concept of the anti-roll bar is to reduce, or even prevent, the rolling effect of the vehicle, which translates into better manoeuvrability depending on the bar used to control rolling stiffness.

Looking at the vehicle in a corner, there will be weight transfer from the inside to the outside of the corner, lifting the inside and compressing the outside, an inevitable rolling situation that occurs in these situations. In general terms, the anti-roll bar is a torsion bar attached to the sprung mass, free to rotate, connected by drop links to the unsprung mass on either side of the vehicle. In this way, using the torsion bar theory, the weight transfer that occurs between the inner wheel and the outer wheel can be reduced, which benefits the vehicle's handling. When both wheels deflect vertically in the same direction, for example when hitting a bump, the antiroll bar only rotates on its supports.

The anti-roll bar not only restricts the rolling tendency of the sprung mass, but also has another aspect of great interest when adjusting the setup, in that it can quickly change the vehicle's balance in terms of understeer/oversteer. In situations of understeer or oversteer, which can easily occur in tests or races, changing the position of the bar or exchanging the anti-roll bar for one with less or more stiffness, quicker and easier than changing springs, for example, will help to correct these behaviours.

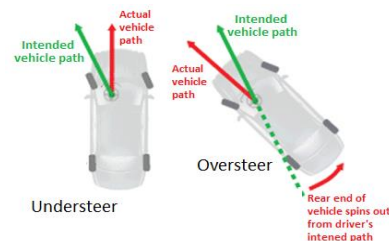


Figure 50 - Understeer vs. Oversteer (Bugeja, Spina, and Buhagiar 2017)

Observing Figure 50, the situation in which the vehicle has low frontal grip leads to understeer behaviour, and one possibility for resolving and correcting this understeer behaviour is to reduce the stiffness of the front axle. Focusing on possible changes to the anti-roll bar to “soften” the front axle, there are three possible situations: either change the front anti-roll bar with lower torsional stiffness, a softer anti-roll bar, or change the working position of the arm (soft, medium, hard), or change the balance by increasing the torsional stiffness on the rear axle, which increases the oversteer effect on the vehicle, counteracting the understeer effect present. Conversely, in an oversteer situation, the opposite logic should be considered. Therefore, reducing the torsional stiffness of the rear anti-roll bar or increasing the torsional stiffness of the front anti-roll bar, can be solutions for handling and improving manoeuvrability.

For this study, the geometry of the Skoda Fabia R5 shown in Figure 51 will be used.

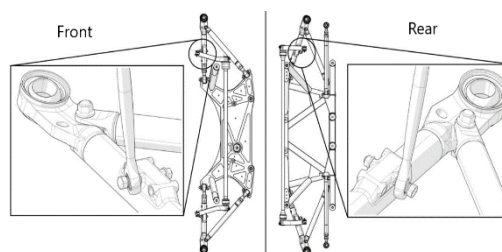


Figure 51 – Anti-roll bar geometry at Skoda (Skoda\_Motorsport 2023b)



Figure 52 shows the three different possible positions for adjusting the anti-roll bar on the front axle and the rear axle, where the anti-roll bar drop link is connected, linking the anti-roll bar to the wishbone arm.

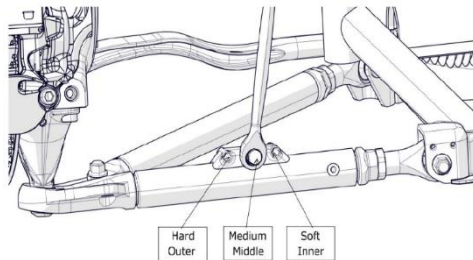


Figure 52 - Adjust system of anti-roll bar (Skoda\_Motorsport 2023b)

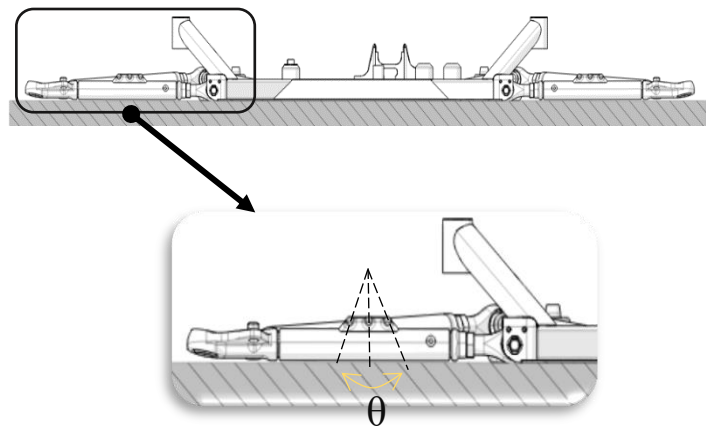


Figure 53 - Theta variation at distinct positions of drop link (Skoda\_Motorsport 2023b)

The position of the drop link is linked to the suspension arm and translates into less or more force being exerted by the anti-roll bar, as the angle of the drop link changes with its vertical projection, Figure 53.

For the study, the rigid system was simplified, since racing vehicles have much greater structural reinforcement than everyday vehicles, using the theory of torsion of the shaft in each bar available for use in the Skoda.

Then, look at Table 2, about the different anti-roll bar diameters at the front and rear of the Skoda Rally2 Evo, all with FIA homologation.

Table 2 - Effective diameter of anti-roll bar Skoda Rally2 Evo (Skoda\_Motorsport 2023b)

Effective diameter	
Front	Rear
16,1	17,7
20,7	21,5
25,5	25,9

During vehicle manoeuvres, particularly when cornering, a torsional force is applied to an anti-roll bar. This torsional force is generated by the fact the wheels on one side of the vehicle suffer a greater vertical load during cornering than the wheels on the other side.

Considering that the system is practically rigid, it is a good approximation to calculate the stiffness of the different bars using equation (2.9), considering the relation  $\frac{M_t}{\theta}$  in Nm/rad.

$$\frac{M_t}{\theta} = G \times I_p \quad (2.9)$$

Where:

$M_t$ , is the torsion moment, in Nm

$\theta$ , is the torsion angle for applied moment, in Rad

$G$ , is the elasticity of the material, in this case is 75.8 GPa

$I_p$ , is Inertia Polar Moment, that will be approximate for a circular section given by equation (2.10),

$$I_p = \frac{\pi \times D^4}{32} \quad (2.10)$$



### 3 Mathematic Modulation

The mathematic modelling of vehicle dynamics is a complex and essential part of understanding how vehicles behave under different conditions and how they can be optimised for various purposes, including improving balance, handling, and achieving optimal performance.

The construction of the corresponding Excel sheet will be presented, which after combining all the information gives us the possibility to carry out dynamic calculations based on the input parameters, to predict the behaviour of a vehicle and analyse the impact of setup changes. Figure 93 in Annexe B shows the cover and main spreadsheet of the tool created in an Excel file.

Vehicle Weights and Dimensions			
Parameter	Units	Value Set1	Value Set2
W1 [FL]	kg	388	388
W2 [FR]	kg	394.5	394.5
W3 [RL]	kg	303	303
W4 [RR]	kg	309	309
<b>Total weight</b>	kg	1394.5	1394.5
Front weight	kg	782.5	782.5
Rear weight	kg	612	612
Weight distribution	% front	56%	56%
	% rear	44%	44%
Front axle unsprung mass	kg	120.4	120.4
Rear axle unsprung mass	kg	122.1	122.1
Front axle sprung mass	kg	662.1	662.1
Rear axle sprung mass	kg	489.3	489.3
Wheelbase	mm	2566	2566
Front Track width	mm	1611	1611
Rear Track width	mm	1606	1606
a	mm	1136.13	1126.13
b	mm	1439.87	1439.87
CG Height	mm	621.80	825.94
Front roll centre height	mm	118.36	118.956
Rear roll centre height	mm	133.45	133.763036
CoG above RC	mm	496.48	700.49
<b>Spring</b>			
Motion ratio - Front	mm/mm	0.821	0.821
Motion ratio - Rear	mm/mm	0.857	0.857
<b>ARB</b>			
Motion ratio - Front	mm/mm	0.379	0.286
Motion ratio - Rear	mm/mm	0.277	0.277
<b>Tyres</b>			
Front Stiffness	N/mm	300,000	300,000
Rear Stiffness	N/mm	300,000	300,000

Weights One Corner			
Parameter - Front	Units	Value Set1	Value Set2
Wheel (Rim+Tyre)	kg	22	22
Complete Hub	kg	16	16
Lower Arm	kg	1.6	1.6
Steering Arm	kg	0.6	0.6
Front Driveshaft	kg	5	5
Damper + Spring	kg	15	15
<b>Total Unsprung Weight</b>	kg	60.2	60.2
<b>Parameter - Rear</b>			
Wheel (Rim+Tyre)	kg	22	22
Complete Hub	kg	16	16
Lower Arm	kg	1.6	1.6
Steering Arm	kg	0.45	0.45
Rear Driveshaft	kg	5	5
Damper + Spring	kg	16	16
<b>Total Unsprung Weight</b>	kg	61.05	61.05

Dimensions Spring			
Parameter - Front	Units	Value Set1	Value Set2
d1 (spring)	mm	480	480
d2 (center contact patch)	mm	560	560
Damper Angle	°	77	77
Angle Correction Factor		0.974	0.974
<b>Parameter - Rear</b>			
d1 (spring)	mm	480	480
d2 (center contact patch)	mm	560	560
Damper Angle	°	78	78
Angle Correction Factor		0.978	0.978

Dimensions ARB			
Parameter - Front	Units	Value Set1	Value Set2
d1 (ARB)	mm	155	155
d2 (center contact patch)	mm	560	560
<b>Parameter - Rear</b>			
d1 (ARB)	mm	212	160
d2 (center contact patch)	mm	560	560
<b>Parameter - Front</b>			
Position	mm	212	160
Wishbone Length	mm	390	390
<b>Parameter - Rear</b>			
Position	mm	155	155
Wishbone Length	mm	390	390

Roll			
Parameter	Units	Value Set1	Value Set2
Roll moment arm	mm	832.841	706.895
Roll Gradient	deg/g	3.500	3.800
Roll Angle	deg	1.000	1.000
Lateral G	G	1.000	1.000

Figure 54 - Excel spreadsheet of input data

Figure 54, shows the spreadsheet that constitutes the start of the calculations with the input parameters that will be needed for the calculations. The yellow-coloured cells that can be seen are the values that need to be entered, and the grey cells are the values calculated for future use. The two columns shown represent the values of two different sets, which are intended for future comparisons of configurations.

Figure 94 in Annexe C shows the paper for recording the measurements needed to fill in the Input Data spreadsheet, to facilitate collection and direct recording.

What's more, each spreadsheet has an information section with formulas, total values, and graphs so that anyone starting to work with the tool in Excel can not only understand the basis of the calculations, but also analyse and understand them in depth, all to help them make decisions.

Figure 55 shows part of the information section for the CG spreadsheet, where the variables are located to help understand the calculations presented later in this chapter. Figure 56, shows part of the information section for the Spring spreadsheet, which contains information on the springs available, in this case from Skoda, and tables of spring stiffness for future help.

Information

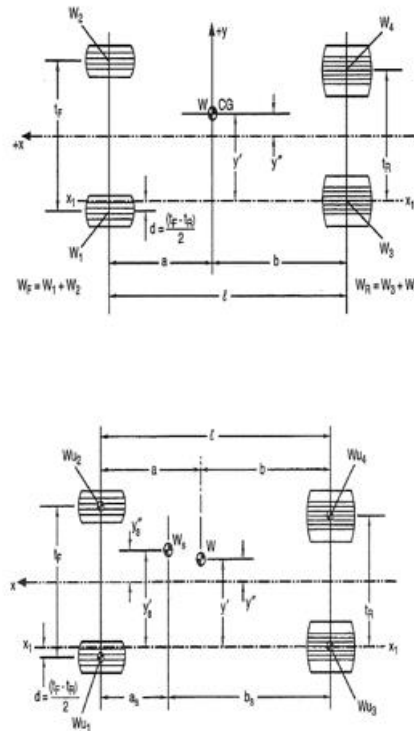
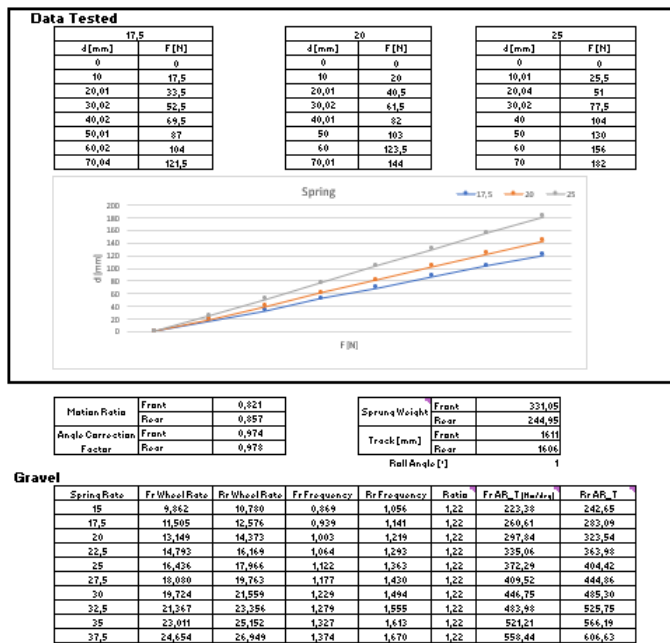


Figure 55 - CG spreadsheet Excel, part of the information section

Information



Spring platform position - Dampers 2021 specification

Side Height [mm]	15,0	17,5	20,0	22,5	25,0	27,5	30,0	32,5	35,0	37,5
max	N/A	N/A	244	241	237	236	233	234	230	232
reference	0	236	241	218	215	211	211	209	209	206
min	-5	230	236	213	210	206	206	204	204	203
max	+25	200	214	196	198	200	203	203	206	205
reference	0	174	189	172	174	175	179	178	183	181
min	-5	169	184	167	169	170	174	174	178	176

Calculated for total weight 1 420 kg and distribution 55 % to front.

Side Height [mm]	30,0	30,0	40,0	40,0	50,0	50,0	60,0	60,0
max	+20	232	233	230	228	N/A min+17 maximum	N/A min+19 maximum	N/A min+19 maximum
reference	0	212	213	210	208	219	217	216
min	-15	196	197	195	193	204	202	201
max	+20	209	214	213	213	225	225	225
reference	0	190	194	194	194	206	206	206
min	-15	174	179	179	179	192	191	191

Calculated for total weight 1 420 kg and distribution 55 % to front.

**Motion Ratio Analysis**

Using the previous analysis and Figure 2, the following apply.

$$K_{\alpha} = K_{\alpha} \left( \frac{a}{b} \right)^2 \cos^2 \alpha$$

- The above analysis assumes minimal camber change at the wheel.
- The motion ratio can be determined experimentally and the measured distance ratio squared for an accurate value.

$$K_{\alpha} = K_{\alpha} \left( \frac{\text{measured along spring axis}}{\text{vertical travel of wheel centerline}} \right)^2$$

Figure 56 - Spring spreadsheet Excel, part of the information section

### 3.1 Location x and y of the CG

To determine the x and y location of the CG, a general case is considered, where the CG is not necessarily on the longitudinal axis, which connects the centre of the front and rear tracks, and the front and rear tracks have different lengths.

Figure 57 shows a diagram of the dimensions and variables used to determine the centre of gravity.

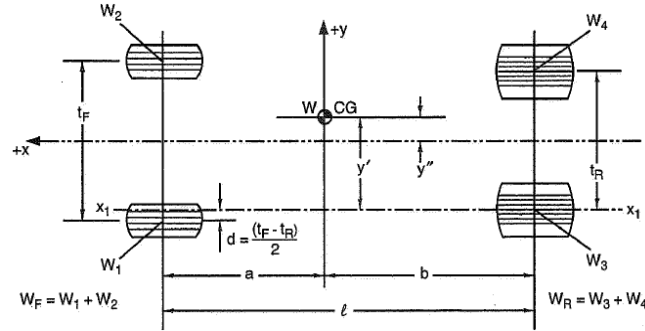


Figure 57 - Centre of gravity location on x and y (William F. Milliken 1995)

The total weight of the vehicle,  $W$ , is the sum of the individual weights of the four wheels, from equation (3.1),

$$W = W_1 + W_2 + W_3 + W_4 \quad (3.1)$$

Considering the moment about the rear axle, equation (3.2),

$$W \cdot b = W_F \cdot l \quad (3.2)$$

$$b = \frac{W_F \cdot l}{W} \quad (3.3)$$

And by determining  $b$  from equation (3.3), can determine  $a$ , equation (3.4),

$$a = l - b \quad (3.4)$$

Consider a line parallel to the axle and passing through the centre of the left rear wheel,  $X_1 - X_1$ , and take the moments of these axes, equation (3.5),

$$W \cdot y' = W_2 \cdot (t_F - d) - W_1 \cdot d + W_4 \cdot t_R \quad (3.5)$$

$$y' = \frac{W_2 \cdot (t_F - d) - W_1 \cdot d + W_4 \cdot t_R}{W} \quad (3.6)$$

For the lateral distance from CG to the centreline,  $y''$  by equation (3.7),

$$y'' = y' - \frac{t_R}{2} \quad (3.7)$$

$$y'' = \frac{W_2 \cdot (t_F - d) - W_1 \cdot d + W_4 \cdot t_R}{W} - \frac{t_R}{2} \quad (3.8)$$

Using equations (3.3), (3.4) and (3.8) the location on the x and y axes is determined.

### 3.2 Vertical Location of the CG

The method for determining the vertical location of the CG is the elevation of the rear at an angle  $\theta$  to the horizontal. The figure is a schematic of the dimension and variables.

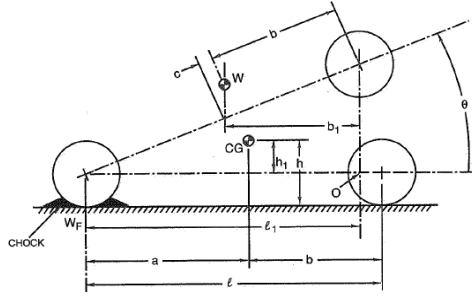


Figure 58 - Vertical location of centre of gravity (William F. Milliken 1995)

With the use of trigonometry, equation (3.9) results  $l_1$ ,

$$l_1 = l \cdot \cos \theta \quad (3.9)$$

Considering the moments of the point O, equation (3.10),

$$W_F \cdot l_1 = W \cdot b_1 \quad (3.10)$$

$$b_1 = \frac{W_F}{W} \cdot l \cdot \cos \theta \quad (3.11)$$

Considering the equations (3.12) and (3.13),

$$\frac{b_1}{b + c} = \cos \theta \quad (3.12)$$

$$c = \left( \frac{W_F}{W} \cdot l \right) - b \quad (3.13)$$

The expression for the vertical location  $h_1$  from equation (3.14),

$$h_1 = \frac{W_F \cdot l - W \cdot b}{W \cdot \tan \theta} \quad (3.14)$$

The final expression for the vertical height from the ground  $h$  from equation (3.15),

$$h = R_{L\ CG} + h_1 \quad (3.15)$$

In which  $R_{L\ CG}$  is the height of the line connecting the centre of the front and rear wheels, defined as equation (3.16),

$$R_{L\ CG} = R_{LF} \left( \frac{b}{l} \right) + R_{LR} \left( \frac{a}{l} \right) \quad (3.16)$$

Where:

$R_{LF}$ , is Front wheel centre height above ground

$R_{LR}$ , is Rear wheel centre height above ground.

### 3.3 Sprung Mass CG Location

With the centre of gravity determined in the previous section, it is also useful to know the location of the centre of gravity of the sprung mass. To calculate this, you need to know the weights of the wheels, tyres, brakes, uprights, arms, drive shafts, springs, and dampers.

#### 3.3.1 Location x and y of sprung mass CG

Considering the general case, shown in Figure 59, with the CG where the total weight of the vehicle is located,  $W$ , have longitudinal location by  $a$  and  $b$  and laterally by  $y'$  and  $y''$ . The sprung weight,  $W_S$ , is located longitudinally as  $a_S$  and  $b_S$ , and laterally as  $y'_S$  and  $y''_S$ .

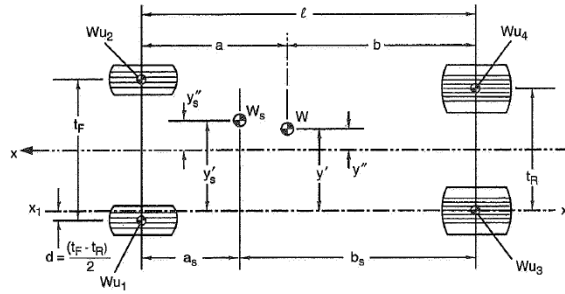


Figure 59 - Sprung mass CG location,  $W_S$  (William F. Milliken 1995)

The sprung weight  $W_S$  corresponds equation (3.17),

$$W_S = W - W_{U1} - W_{U2} - W_{U3} - W_{U4} \quad (3.17)$$

The front unsprung weight is equation (3.18),

$$W_{UF} = W_{U1} + W_{U2} \quad (3.18)$$

And the rear unsprung weight is equation (3.19),

$$W_{UR} = W_{U3} + W_{U4} \quad (3.19)$$

Equation (3.20), which corresponds to the moments about the rear axle, and equation (3.21) are used to determine the longitudinal position of the CG sprung mass,

$$b_S = \frac{W_b - W_{UF} \cdot l}{W_S} \quad (3.20)$$

$$a_S = l - b_S \quad (3.21)$$

Using the same method as for the lateral location of the centre of gravity, the lateral location of the sprung mass CG is determined from equation (3.22),

$$y'_S = \frac{W \cdot y' - W_{U2} \cdot (t_F - d) - W_{U4} \cdot t_R + W_{U1} \cdot d}{W_S} \quad (3.22)$$

And the distance from the centre line,  $y''_S$  from equation (3.24),

$$y''_S = y'_S - \frac{t_R}{2} \quad (3.23)$$

$$y''_S = \frac{W \cdot y' - W_{U2} \cdot (t_F - d) - W_{U4} \cdot t_R + W_{U1} \cdot d}{W_S} - \frac{t_R}{2} \quad (3.24)$$

### 3.3.2 Vertical Location of sprung mass CG

The process for determining the height of the centre of gravity of the sprung mass is more straightforward than for the centre of gravity of the total weight. Figure 60 shows the dimensions and variables required to determine  $h_S$ .

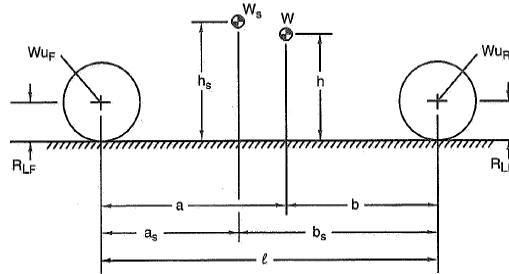


Figure 60 - Height of sprung mass centre of gravity (William F. Milliken 1995)

Taking the moments about the ground,  $h_S$  is equation (3.25),

$$h_S = \frac{W \cdot h - W_{UF} \cdot R_{LF} - W_{UR} \cdot R_{LR}}{W_S} \quad (3.25)$$

### 3.4 Excel - Centre of Gravity

Once the equations needed to calculate the location of the centre of gravity and the centre of gravity of the sprung mass have been presented, respectively, in the previous chapters, they are organised in excel and the calculation can be carried out. Figure 61 shows the weights of the two different configurations that are considered. Also, the values of the inputs, which come from the input spreadsheet and, on the right-hand side, the values of the calculation results.

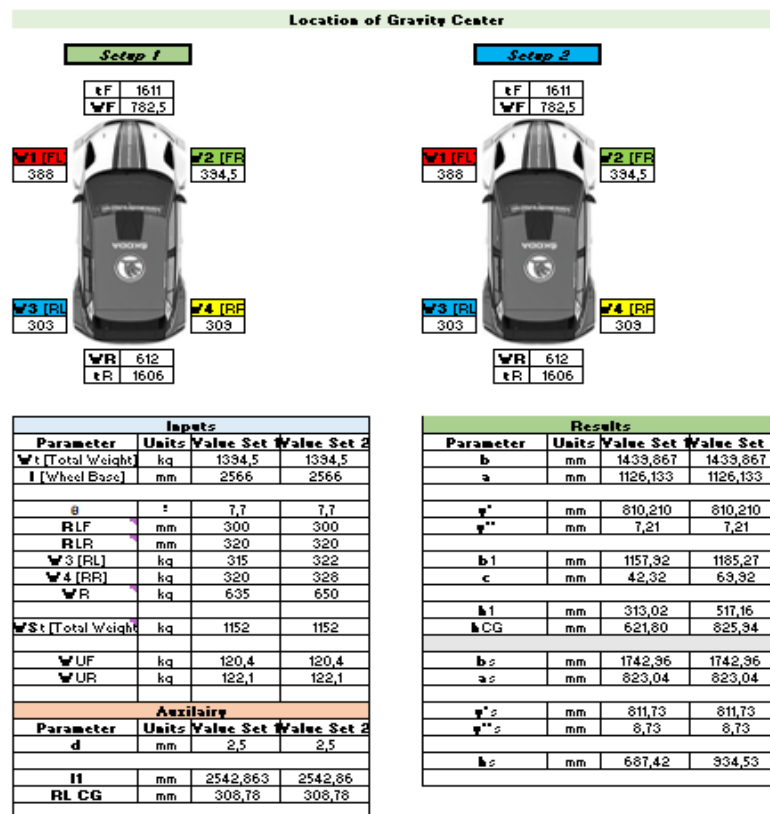


Figure 61 - Excel spreadsheet, Centre of Gravity

In the same spreadsheet as the location of the centre of gravity, there are also calculations for the height of the roll centre. Figure 62 shows the information on the roll centre points on the right-hand side, as well as the input values, auxiliary calculations and finally the respective roll centre height value in the table on the left-hand side.

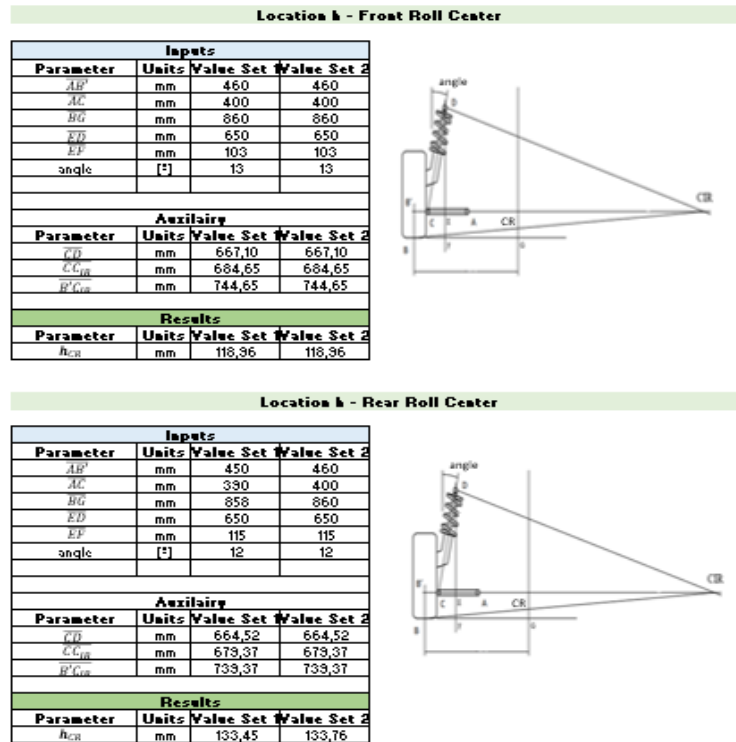


Figure 62 - Excel spreadsheet, Centre of Gravity - Roll centre height calculation

### 3.5 Roll Rates

In order to be able to understand the normal force on the wheel with the position of the wheel in relation to the body, it is necessary to calculate the roll rate.

The total roll rate  $K_{\phi}$  is the contribution of the roll rates of the tires, springs, and anti-roll bar, given by equation (3.26),

$$K_{\phi} = K_{\phi T} + K_{\phi S} + K_{\phi B} \tag{3.26}$$

Where:

- $K_{\phi}$  is the vehicle roll rate
- $K_{\phi T}$  is the tyres roll rate
- $K_{\phi S}$  is the spring roll rate
- $K_{\phi B}$  is the anti-roll bar roll rate.

Relating the installation ratio explained above on 2.2 Suspension Geometry, which affects the spring force and displacement, with the attention that it must be raised to 2 to be able to relate the wheel centre ratio to the spring ratio, from equation (3.27).

$$K_W = K_S IR^2 \tag{3.27}$$



Where:

$K_W$  is the wheel centre rate

$K_S$  is the spring rate

IR is the installation ratio

Taking a natural frequency from the literature that should be normal for this type of vehicles, referring to the book Milliken & Milliken, where the value is 1.5 Hz. With this assumption it is possible to calculate the ride rate,  $K_R$ , according to equation (3.28).

$$K_R = 4\pi^2 \omega^2 \frac{m_S}{2} \quad (3.28)$$

Where:

$m_S$  is the sprung mass.

To calculate the wheel centre rate, the ride rate can be seen as two springs in series, one acting between the body and the wheel, wheel centre rate, and the other acting between the wheel and the ground, tire rate, shown in equation (3.29).

$$K_W = \frac{K_R K_T}{K_T - K_R} \quad (3.29)$$

With equation (3.30), obtain the spring rates,

$$K_S = \frac{K_W}{IR^2} \quad (3.30)$$

The spring roll rate is obtained from equation (3.31),

$$K_{\phi S} = \frac{K_R T^2}{2} \quad (3.31)$$

Follow the tires roll rate, equation (3.32),

$$K_{\phi T} = \frac{K_T T^2}{2} \quad (3.32)$$

For the contribution of the anti-roll bar to the roll rate is given by the equation (3.33),

$$K_{\phi B} = K_{\theta B} I_B^2 \left( \frac{T^2}{L^2} \right) \quad (3.33)$$

Where:

$K_{\phi B}$  is the contribution of the anti-roll bar for the total vehicle roll rate

$K_{\theta B}$  is the anti-roll bar roll rate

$I_B$  is the installation ratio of the anti-roll bar

L is the anti-roll bar dimension

T is track dimension.

It is necessary to explain at this point that, for the anti-roll bar rate, it is necessary to convert the anti-roll bar stiffness, which is in Nm/rad units, to the same units as the spring and tyre rate, N/mm, for which the wishbone ratio shown in Figure 63 is used.

Wishbone Ratio			
Parameter - Front	Units	Value Set1	Value Set2
Soft	mm/mm	0,410	
Medium	mm/mm	0,477	
Hard	mm/mm	0,544	

Wishbone Ratio			
Parameter - Front	Units	Value Set1	Value Set2
Soft	%mm	0,115	
Medium	%mm	0,133	
Hard	%mm	0,152	

Wishbone Ratio			
Parameter - Rear	Units	Value Set1	Value Set2
Soft	mm/mm	0,397	
Medium	mm/mm	0,464	
Hard	mm/mm	0,531	

Wishbone Ratio			
Parameter - Rear	Units	Value Set1	Value Set2
Soft	%mm	0,111	
Medium	%mm	0,130	
Hard	%mm	0,148	

Figure 63 - Wishbone ratio

With the contribution of all the elements defined for the vehicle's total roll rate, it is possible to predict the vehicle's behaviour in terms of cornering and handling performance.

### 3.6 Excel - Mechanical Balance

The previous chapter, point 3.5, presented the equations for the wheel rate, spring rate, and anti-roll bar rate, and these contribute to the vehicle's total roll rate. Figure 64 shows the rate values on the left-hand side, and in the green-coloured cells at the bottom are the total front and rear rates.

On the right-hand side of the figure are the calculation for roll rate, suspension roll stiffness, and angular stiffness. These calculations are for a deeper understanding of the vehicle's behaviour and for future development.

Roll Rate			
Parameter	Units	Value Set1	Value Set2
Front Roll Stiffness / Roll Rate	Nm/rad	57337,98	34945,44
Rear Roll Stiffness / Roll Rate	Nm/rad	51200,11	33829,32

Suspension Roll Stiffness			
Parameter	Units	Value Set1	Value Set2
Front Roll Stiffness / Roll Rate	Nm/l	1,17	1,17
Rear Roll Stiffness / Roll Rate	Nm/l	1,03	1,03

Stiffness			
Parameter	Units	Value Set1	Value Set2
Front Angular Stiffness	Nm/l	1000,66	999,24
Rear Angular Stiffness	Nm/l	893,54	893,54
Angular Stiffness	Nm/l	1894,21	1892,79
Roll Stiffness	°/G	3,59	5,06

Roll			
Parameter	Units	Value Set1	Value Set2
Roll Lateral Moment	Nm/g	564,970	794,336
Roll Gravity Moment	Nm/g	34,512	52,682
Roll Moment	Nm/g	599,482	847,019
Front Anti Roll Torque Spring	Nm/rad	595,67	670,13
Rear Anti Roll Torque Spring	Nm/rad	647,07	647,07

Rates			
Parameter	Units	Value Set1	Value Set2
Front tire rate	N/mm	300,00	300,00
Rear tire rate	N/mm	300,00	300,00
Front Spring rate	N/mm	40,00	45,00
Rear Spring rate	N/mm	40,00	40,00
Front Wheel rate [No ARB]	N/mm	26,30	29,59
Rear Wheel rate [No ARB]	N/mm	28,75	28,75
Front Ride Rate [No ARB]	N/mm	24,18	26,93
Rear Ride Rate [No ARB]	N/mm	26,23	26,23
Front ARB rate	N/mm	11,82	6,73
Rear ARB rate	N/mm	5,76	5,76
Front Spring + ARB Rate	N/mm	51,82	51,73
Rear Spring + ARB rate	N/mm	45,76	45,76
<b>Front Total Rate</b>	N/mm	<b>44,19</b>	<b>44,12</b>
<b>Rear Total Rate</b>	N/mm	<b>39,70</b>	<b>39,70</b>
		<b>52,67%</b>	<b>52,64%</b>

Figure 64 - Excel spreadsheet, Mechanical Balance

### 3.7 Wheel Load under constant Braking

When acceleration is applied to the vehicle to push it forwards, a longitudinal force arises in the drive wheels. In order for the vehicle to be in balance, a force that reacts with this longitudinal force,  $ma_x$ , is considered at the centre of gravity, as shown in Figure 65.

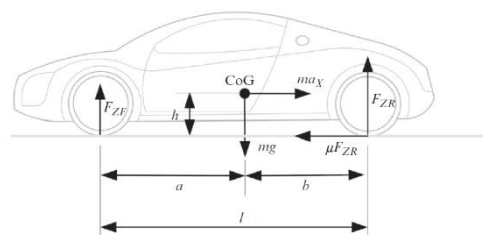


Figure 65 - Free-body diagram for acceleration(Balkwill 2018a)

Taking the moments in the rear contact patch, equation (3.34),

$$F_{ZF} \cdot l + ma_x \cdot h = mg \cdot b \quad (3.34)$$

$$F_{ZF} = \frac{mg \cdot b - ma_x \cdot h}{l} \quad (3.35)$$

By a similar process, taking the moments on the front contact patch, result equation (3.36),

$$F_{ZR} = \frac{mg \cdot a + ma_x \cdot h}{l} \quad (3.36)$$

Equations (3.35) and (3.36) show that during vehicle acceleration, the load on the front tyres decreases and the load on the rear tyres increases by the same amount. The total load remains constant, so the load lost at one end is the same as that gained at the other. It should be noted that this transfer of weight is a fundamental effect in driving and that the vehicle's suspension, dampers, and springs, affect the transfer of weight from the front to the rear when accelerating or from the rear to the front when braking.

### 3.8 Wheel Loads Under Cornering

As seen in the previous section on longitudinal acceleration, point 3.7, a similar analysis can be prepared for lateral acceleration by drawing a balance diagram, shown in Figure 66.

The centripetal force,  $ma_y$ , is acting on the centre of gravity and is in balance with the lateral forces  $\mu F_{Zl}$  and  $\mu F_{Zo}$ .

Considering a rigid chassis model for the analysis to obtain the equations and not considering the weight transfer between the front and rear during cornering.

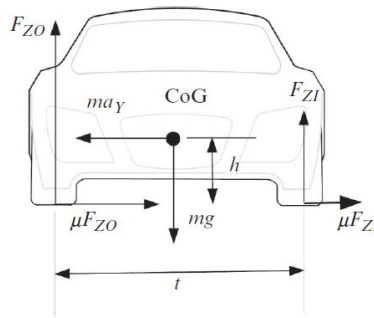


Figure 66 - Free body diagram on cornering (Balkwill 2018b)

With the moment about the contact patch on the inner wheel, equation (3.37),

$$F_{ZO} \cdot t = mg \cdot \frac{t}{2} + ma_y \cdot h \quad (3.37)$$

$$F_{ZO} = \frac{mg}{2} + \frac{ma_y \cdot h}{t} \quad (3.38)$$

Similarly, equation (3.39) results for the outer wheel,

$$F_{Zl} = \frac{mg}{2} - \frac{ma_y \cdot h}{t} \quad (3.39)$$

From equations (3.38) and (3.39), it can be concluded that, when cornering, the load will be higher on the outer wheels than on the inner wheels. Furthermore, as in the longitudinal case, the amount of weight transferred depends only on the height of the centre of gravity to the ground, rather than the wheelbase in the longitudinal case, and has no influence on the suspension characteristics.

### 3.9 Excel - Weight Transfer

One of the last calculations, after looking at the calculations for the centre of gravity, the roll centre height, and the roll stiffness, is the longitudinal and lateral weight transfer. The calculations used in the Excel have a linear behaviour, which is not reality, but is an approximation to give an understanding of how weight transfer occurs.

The calculations made and the organisation of the Excel spreadsheet are shown in Figure 67.

On the left-hand side, in the tables labelled yellow, are the calculations for longitudinal load transfer and the suspension's contribution to anti-roll. In the green heading are the lateral load transfers with the contribution of the components and, at the end, the total wheel loads.

On the right-hand side, for a better understanding and a more direct approach, there is a figure of the vehicle with the initial weight at first, then the weight after the load transfer and finally the difference to the other values.

Longitudinal load transfer and its components			
Parameter	Units	Value Set1	Value Set2
Front axle static weight	kg	782,5	782,5
Rear axle static weight	kg	612	612
Longitudinal load transfer	kg	327,318	443,860
Front axle weight after load	kg	444,552	333,640
Rear axle weight after load transfer	kg	943,318	1060,860

Anti Roll Contribution			
Parameter	Units	Value Set1	Value Set2
Front AR K Springs	Nm/°	535,670	670,123
Rear AR K Springs	Nm/°	647,073	647,073
Total AR K Springs	Nm/°	1242,744	1317,202
Front AR K ARB	Nm/°	535,357	204,338
Rear AR K ARB	Nm/°	259,195	253,195
Total AR K ARB	Nm/°	794,552	564,133
Total AR K	Nm/°	2037,296	1881,335

Sprung Mass Roll			
Parameter	Units	Value Set1	Value Set2
SM Roll Angle	°	2,783	4,247
SM roll Gradient	°/G	2,783	4,247

Lateral Load Transfer			
Parameter	Units	Value Set1	Value Set2
Front NSM	kg	17,750	14,237
Rear NSM	kg	18,057	14,483
Front Elastic	kg	139,621	262,021
Rear Elastic	kg	160,450	244,231
Front Geometric	kg	48,883	48,883
Rear Geometric	kg	40,703	40,804
Total Front	kg	266,261	325,147
Total Rear	kg	219,216	239,578

Lateral Load Transfer Contribution			
Parameter	Units	Value Set1	Value Set2
NSM	%	7,38	4,60
Elastic	%	74,17	81,05
Geometric	%	18,456	14,357

Lateral Load Transfer Distribution			
Parameter	Units	Value Set1	Value Set2
NSM	%	43,57	43,57
Elastic	%	55,44	51,75
Geometric	%	54,57	54,51
Total	%	54,85	52,05

Wheel Loads			
Parameter	Units	Value Set1	Value Set2
FL	kg	124,33	66,10
FR	kg	651,51	716,40
RL	kg	216,22	6,42
RR	kg	525,22	605,58

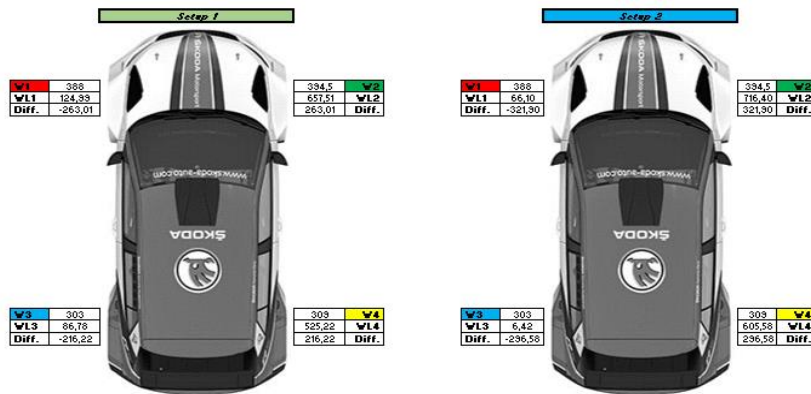


Figure 67 - Excel spreadsheet, Weight Transfer

To illustrate the transfer of weight in relation to lateral acceleration, Figure 68 shows the relationship between the calculations presented above and the approximation to linear behaviour.

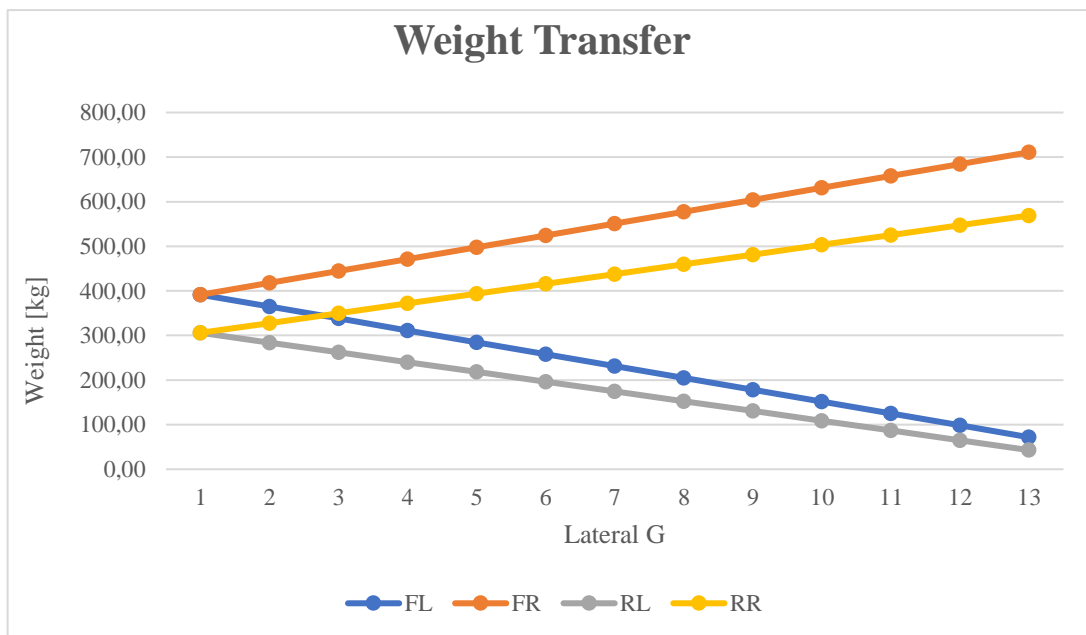


Figure 68 - Weight transfer graphic

## 4 Procedure and Solution

This chapter will present the procedures, the data relevant to the development and the results obtained. All the information described so far in the previous chapters serves as the basis and foundation for this chapter.

### 4.1 Previous Vehicles Analyses

Based on previous analyses, an initial approach should be understood, starting with the approval book and the geometric survey points. It should be borne in mind that the geometric survey points are not entirely free of error, due to the difficulty of access.

In this way, the information shown in Table 3 was taken from the approval book delivered by the manufacturer.

Table 3 - Data from homologation book (Skoda\_Motorsport 2023a)

<b>Main dimensions</b>		
<b>Parameter</b>	<b>Unit</b>	<b>Value</b>
Overall Length	mm	4108
Overall Width	mm	1820
Front Width (middle tyre)	mm	1356
Rear Width (middle tyre)	mm	1340
<b>Unsprung Weight</b>		
<b>Parameter</b>	<b>Unit</b>	<b>Value</b>
Wheel and Rim	Kg	22,00
Hub Carrier	Kg	16,00
Complete Front Wishbone/arm	Kg	3,06
Front Toe Link	Kg	1,20
Rear Toe Link	Kg	0,876

The dimensions and weights required for the initial calculations were carried out three times and the average value was taken as the value to be used as input. The aim is to obtain the most accurate results possible. The following subchapters present the respective measurements taken, the calculations and a brief analysis of the values.

### 4.2 Mass Distribution

To determine the vehicle's mass distribution, four individual scales were used, one at each corner of the vehicle, on platforms to have a complete ground plane, as shown in Figure 69. In this figure you can see the 4 scales that make up the desired flat bottom and the use of a lift, which is used to slowly lower the vehicle onto the scales. The respective weight at each corner was recorded and the horizontal position of the centre of gravity was calculated.

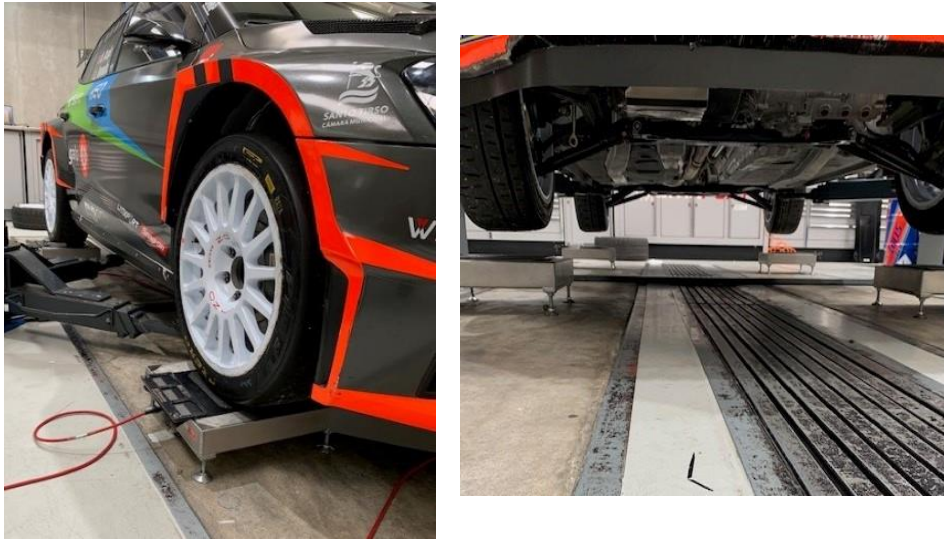


Figure 69 - Platforms with scales to create the plan ground

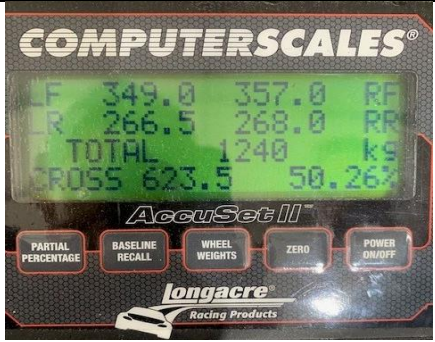
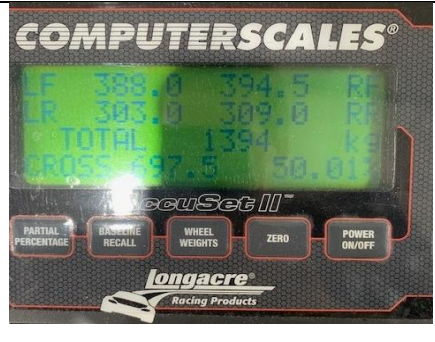
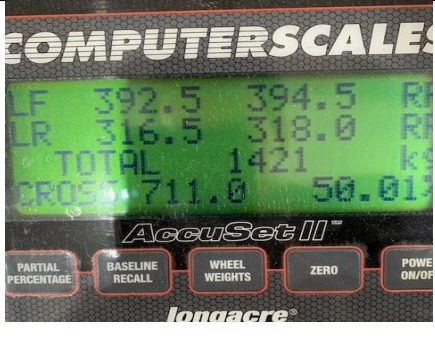
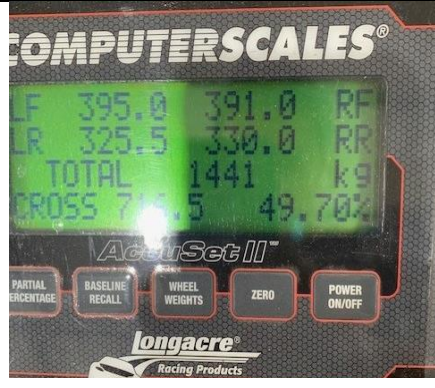
To understand the different distribution of the weights and the notion of how the weights move, in static considerations, different stages were carried out and the different weights at each corner during the different stages were recorded. This also gives us an idea of how the distribution of weights occurs during the race and the need to balance the weights during the stages of the race. For example, on a super special stage, the fuel level will be as low as possible, so taking into account the measurements made in the workshop, the weight of the car with the divers will be observed and taken into account, which is very close to reality. Or, considering a morning stage where more fuel is needed, and then it is observed how the static weight is affected and the changes that can be considered.

With the scale at zero, the vehicle was lowered, the brake was applied so that the vehicle would not follow the scale and the vehicle was then oscillated to overcome the resistance of the mechanical elements and reach the correct height. The weights were only recorded in one measurement, because if the vehicle was lifted it would alter the measurement of the weights, so only one measurement was taken so that the weights were controlled as well as possible to be able to reproduce the procedure with the least error. There is the error of the scales, with the slight movement of the car the weights change, if the height is not the same as before, all these considerations lead to different values. To do this, the vehicle was lowered once, its weight recorded, and the different weights added with as little disturbance as possible.

Table 4 below shows the steps and weights recorded at each corner, where the respective value of that measure is present.



Table 4 - Weights considering different steps

<p>1° - was weight with guards and ballast, Figure 70</p>	 <p>Figure 70 - Weight of car, with guards and ballast</p>
<p>2° - was weight with the driver and co-driver, 77kg each one, Figure 71</p>	 <p>Figure 71 - Weight with driver and co-driver</p>
<p>3° - was weight with the addition of 35L of fuel, Figure 72</p>	 <p>Figure 72 - Weight with addition of 35L of fuel</p>
<p>4° - was with addition of the second spare tyre, Figure 73</p>	 <p>Figure 73 - Weight with addition of second spare tyre</p>

This data is used to understand how the centre of gravity changes in different conditions, so that you can better understand its movement when weights are added to the car. But also, to know how the static weight of the vehicle is, which is considered for different stages of the event, whether it's a test or a race.

#### 4.2.1 Horizontal Centre of Gravity

With the difference in weights recorded in the previous chapter, point 4.2, you can see the changes in the horizontal measurement of the centre of gravity and how it moves with the weights. These changes are shown below in Table 5, where you can see the a-measure (front axle to CG) and the b-measure (rear axle to CG) for the different steps.

Table 5 - Location of x and y of the centre of gravity on this specific case

<b>Location of x and y of the CG</b>			
Condition	a [mm]	b [mm]	y'' [mm]
1° - Weight with guards and ballast	1106	1146	6
2° - Weight with addition of driver and co-driver	1126	1440	7
3° - Weight with addition of 35L of Fuel	1145	1421	2
4° - Weight with addition of the second spare tyre	1167	1399	0

From the table you can see and consider some conclusions about the impact of weight on the location of the centre of gravity. With the addition of weight, the movement of the centre of gravity has the expected behaviour of moving closer to the centre, and with the first measurement most of the weight is found at the front by the engine and gearbox, which gives us a CG measurement closer to the front axle. The addition of the weight of the driver and co-driver is more central, as is that of the fuel, which moves the CG away from the frontal axis and closer to the centre of the vehicle. The last measurement with the second spare tyre, which is at the rear of the vehicle, had the same effect of increasing the distance between the CG and the front axle, i.e., closer to the centre in longitudinal terms. It can be seen that from the first measurement to the fourth, point a has been moving away from the front axle, which has the effect of making the car less understeering, meaning a more neutral car, which is one of the main objectives. It can also be seen that the centre of gravity, with the addition of the weight, moves closer to the central axis of the car in the y'' measurement, which has an effect on the lateral transfer of weight during cornering.

From these measurements it is possible to look at another perspective, which is the alteration of the front and rear guards to shift the weight further forwards or backwards and have the notion that even without a real value the knowledge behind the alteration is understood and can be used to predict the vehicle's handling.

#### 4.2.2 Vertical Centre of Gravity

The methodology described in chapter 3.2 Vertical Location of the CG was used to calculate the height of the centre of gravity.

However, a change was made to this methodology, which was to raise the front axle, as seen in the Figure 74, because it has more weight than the rear axle. It's not a big difference, but the aim is to reduce errors as much as possible in order to get the most accurate values.



Figure 74 - Elevation of the vehicle

The height of the centre of gravity only registered with the weight of the driver and co-driver and then when the 35 litres of fuel were added. It was only possible in these two conditions and due to the limited time, only one measurement was taken, however, it should be repeated, and more measurements taken so that the values are more correct, since carrying out this process of lifting the front end, although it seems simple, is complicated by avoiding errors and inaccurate measurements.

With the weights recorded and the degree of inclination of the car for the calculations also recorded, the input values were submitted in Excel's CG tab and the results for the height of the centre of gravity and the height of the centre of gravity of the sprung mass were obtained and shown in Table 6.

Table 6 - Location of height of the centre of gravity

<b>Location of h of the CG</b>		
Condition	$h$ [mm]	$h_s$ [mm]
2° - Weight with addition of driver and co-driver	622	687
3° - Weight with addition of 35L of Fuel	826	935

### 4.3 Instantaneous centre and roll centre

The determination of the instantaneous centre was realized taking with the vehicle at rest on top of the plan ground obtain for the calibration of 4 platforms for the alignment. Having

this in consideration the following points was tacked, present on Table 7. With the scheme of the points on Figure 75 and the real view on Figure 76.

Table 7 - Measurement points for front roll centre

Parameter	Units	Value
$\overline{AB}$	mm	460
$\overline{AC}$	mm	400
$\overline{BG}$	mm	860
$\overline{ED}$	mm	650
$\overline{EF}$	mm	105
Angle	degrees	13

It should be noted that the distance  $\overline{EF}$  is the ride height of the vehicle from the ground, considering the recommendation of Skoda.

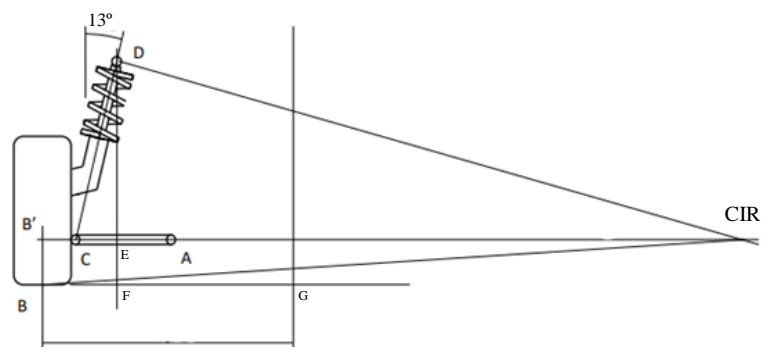


Figure 75 - Scheme of suspension measures

With the values obtained from the measures it was proceed the calculations that are presented on the Table 8. The Figure 75 and Figure 76 help to understand these calculations and the points described to achieve the roll centre height.



Figure 76 - Suspension elements and measure process

Table 8 - Suspension measures for calculation of the front roll centre height

Points	Calculation
$\overline{CD}$	$\frac{\overline{DE}}{\cos(13^\circ)} \Leftrightarrow \overline{CD} = 667 \text{ mm}$
$\overline{CCIR}$	$\frac{\overline{CD} * \sin(90^\circ)}{\cos(13^\circ)} \Leftrightarrow \overline{CCIR} = 685 \text{ mm}$
$\overline{B'CIR}$	$\overline{CCIR} + (\overline{AB'} - \overline{AC}) \Leftrightarrow \overline{B'CIR} = 745 \text{ mm}$
$h_{CR}$	$\frac{\overline{EF} * \overline{BG}}{\overline{B'CIR}} \Leftrightarrow h_{CR} = 119 \text{ mm}$

At static suspension and with this specific setup the roll centre height is 118,96 mm from the ground on the front axle.

On the rear axle, the process is similar to that of the front axle, as it is also a McPherson strut. The dimensions required for the rear roll centre height calculations were recorded, as presented on Table 9, and the results obtained are presented on Table 10.

Table 9 - Measurement points for rear roll centre

Parameter	Units	Value
$\overline{AB}$	mm	450
$\overline{AC}$	mm	390
$\overline{BG}$	mm	858
$\overline{ED}$	mm	650
$\overline{EF}$	mm	115
<i>Angle</i>	degrees	12

Table 10 - Suspension measures for calculation of the rear roll centre height

Points	Calculation
$\overline{CD}$	$\frac{\overline{DE}}{\cos(13^\circ)} \Leftrightarrow \overline{CD} = 664,52 \text{ mm}$
$\overline{CCIR}$	$\frac{\overline{CD} * \sin(90^\circ)}{\cos(13^\circ)} \Leftrightarrow \overline{CCIR} = 679 \text{ mm}$
$\overline{B'CIR}$	$\overline{CCIR} + (\overline{AB'} - \overline{AC}) \Leftrightarrow \overline{B'CIR} = 739 \text{ mm}$
$h_{CR}$	$\frac{\overline{EF} * \overline{BG}}{\overline{B'CIR}} \Leftrightarrow h_{CR} = 134 \text{ mm}$

Using the same logic as for the front axle, with static suspension and this particular configuration, the roll rear centre height is 133,45 mm from the ground.

Up to this point, the geometric coordinates of the centre of gravity and the respective heights of the front and rear roll centres have been presented. This is the basis for moving on to calculations relating to longitudinal and lateral load transfer and understanding roll rates.

With this in mind, it is possible to understand the mechanical balance of the vehicle, to give a mathematical value for the configuration used and to make comparisons with changes in vehicle behaviour.

It should be noted that this mathematical process is carried out in static mode, but when it comes to dynamics, the movement of the vehicle itself is not linear and this process must be taken into consideration.

#### 4.4 Ride and Roll Characteristics

The analysis is based on the method presented in chapter 3.4 Roll Rates. Given the numerous springs and anti-roll bars solutions with different attachment positions, a solution for the dynamic behaviour is presented here. This is obtained using Microsoft Excel software, where the different values of interest are automated by changing the springs, anti-roll bar or position.

To better understand the effect of the different springs and anti-roll bars available, in this case for the Skoda Fabia Rs Rall2, a small study was carried out on each element to determine how it behaves and how it changes.

##### 4.4.1 Springs Characteristics

Firstly, the study carried out on the springs is presented, in particular the asphalt springs, where the spring rate, frequency and anti-roll torque can be seen. Note that the spring rate is linear with the three graphs, showing a similar behaviour.

Figure 77, Figure 78 and, Figure 79 show similar behaviour with a linear progression as the spring rate increases. It can also be seen that the rear values are slightly higher than the front values. This can be explained by the need for the rear to have a different dynamic behaviour, for example when the vehicle goes over a bump.

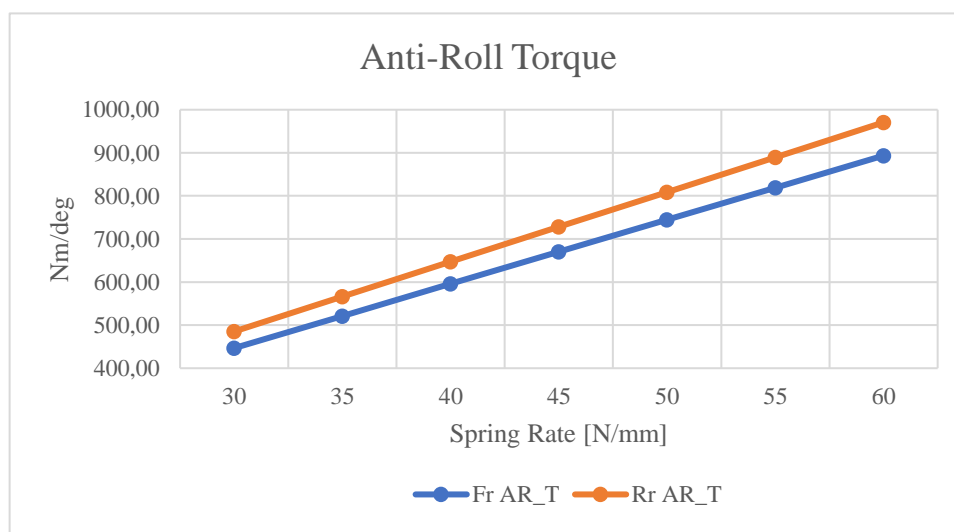


Figure 77 – Anti-Roll torque for tarmac springs

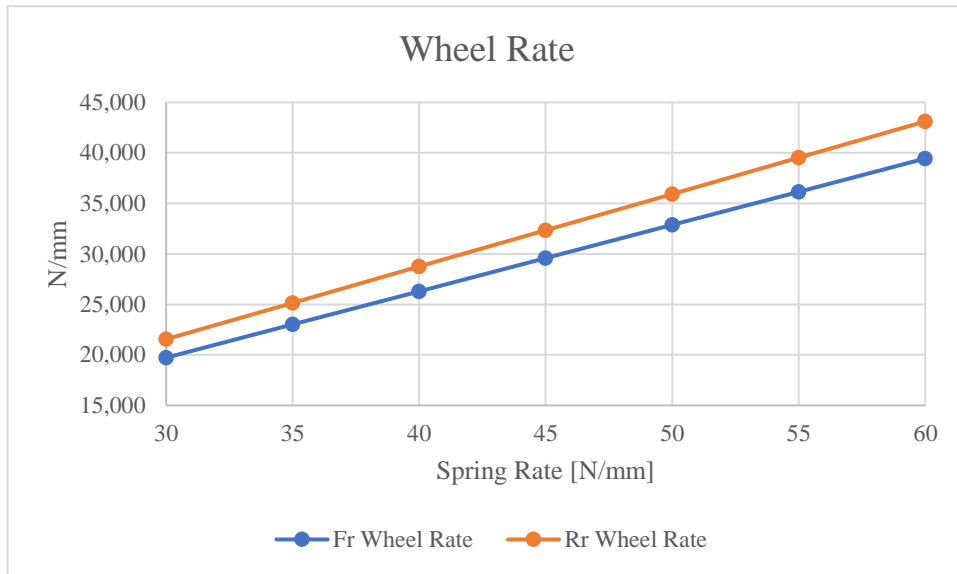


Figure 78 - Wheel rate graphic for tarmac springs

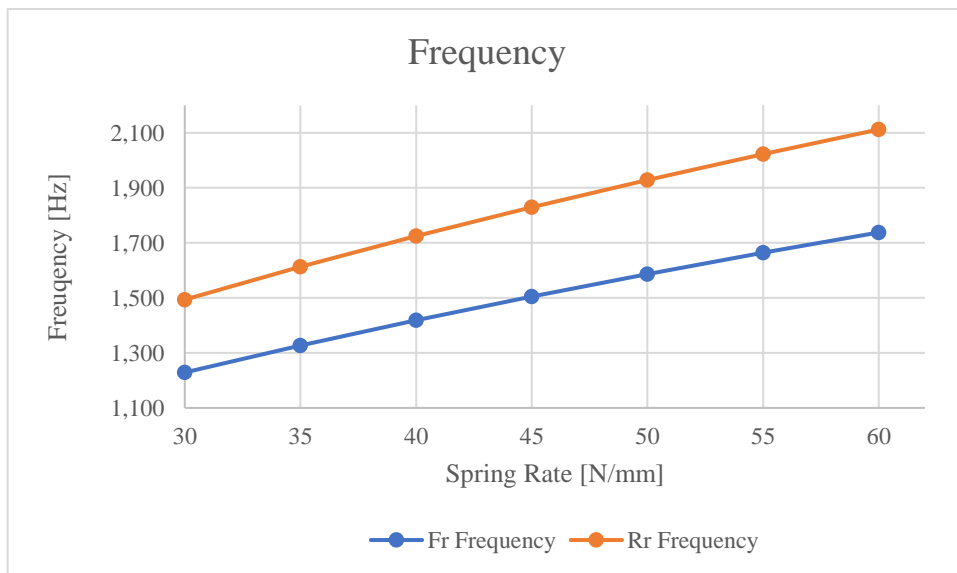


Figure 79 - Frequency for the tarmac springs

Looking at Figure 79, which shows the spring frequencies at the front (blue) and rear (orange). You can see that the rear has a higher frequency, i.e. a stiffer frequency than the front. The purpose of this difference is what is known as "flat ride", because when the front goes over a bump and only after a certain time does the rear go over the bump, depending on the speed, it is intended that the rear should settle at the same time as the front, which is why this difference in frequencies is necessary.

#### 4.4.2 Anti-roll Bar Characteristics

Studying the anti-roll bar was a more complex process, as there is not only the torque of the bar but also the different positions in which the arm can be tightened. For the bar torque, the equation in subchapter 2.14 Anti-roll bar for each different diameter was used, and with this value and the ratio of the wishbone for the different positions, the values for the different rates of the anti-roll bar could be obtained. Table 11 and Table 12 show the results for the front and rear anti-roll bars respectively.



Table 11 - Front ARB rates for the different diameters and positions

Front ARB Calculation				
Parameter	Units	17,3	21,8	26,3
Stiffness	Nm/rad	666,58	1680,72	3560,35
Inner	N/mm	2,67	6,73	14,26
Middle	N/mm	3,61	9,10	19,27
Outer	N/mm	4,69	11,82	25,03

Table 12 - Rear ARB rates for the different diameters and positions

Rear ARB Calculation				
Parameter	Units	17,7	21,3	25,2
Stiffness	Nm/rad	730,40	1531,75	3001,04
Inner	N/mm	2,75	5,76	11,28
Middle	N/mm	3,74	7,85	15,38
Outer	N/mm	4,90	10,27	20,12

For a better understanding and visualisation of the values presented in the tables above, they have been illustrated in graphs and shown in Figure 80 and Figure 81 below, respectively for the front and rear anti-roll bar.

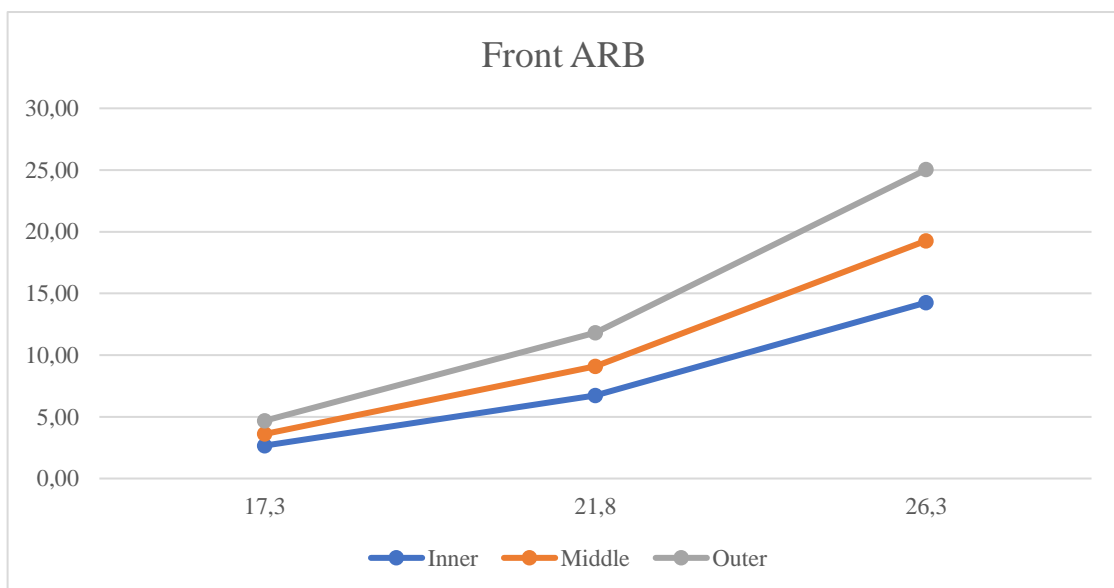


Figure 80 - Front ARB for the different diameters and positions



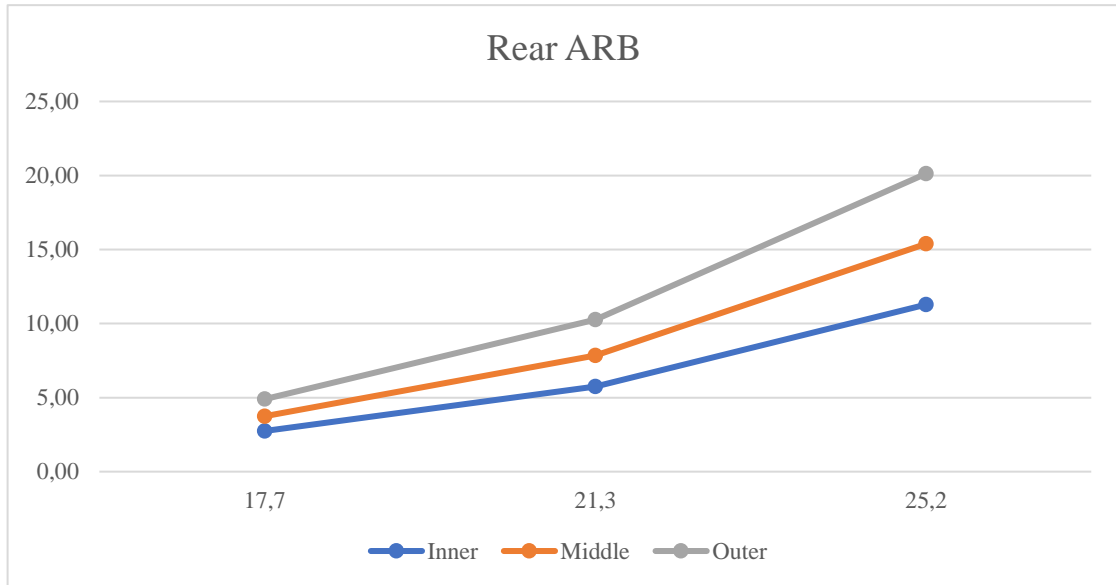


Figure 81 - Rear ARB for the different diameters and positions

It can be seen from the graphs that the behaviour is not completely linear, with a stiffness step in the bar with the largest diameter, which can be translated into a percentage value by looking at the stiffness ratio in Table 13.

Table 13 - Percentage increase in the torsional stiffness modulus

ARB		D [mm]	Mt/θ [Nm/rad]	%
Front	Soft	17,3	666,58	-
	Medium	21,8	1680,72	40%
	Hard	26,3	3560,35	47%
Rear	Soft	17,7	730,40	-
	Medium	21,3	1531,75	48%
	Hard	25,2	3001,04	51%

Looking at the front ARB, you can see that from the soft bar to the medium bar there is a 40 per cent increase in stiffness and from the medium bar to the hard bar, the bar with the largest diameter, there is a 47 per cent increase in stiffness.

This comparison in terms of percentage of stiffness and the stiffness ratio for each position offers help in setting change decisions, but also understands whether the step change will be significant or gives a prediction of the feeling the driver will discuss after the race.

All this information that can be collected to give confidence and more certainty in the changes is fundamental for the behaviour to be understood in values and not just in driver comments and visual aspects.

To help the decision even more, the Table 14 shows the distribution of the bearing for the position of the front bar, which in this case the Inner, that can be changed to give values for the other two positions, in relation to the hypotheses available for the rear anti-roll bar in percentage values.

Table 14 - Roll distribution in ARB, with consideration front position

			Front Antiroll Bar			
		Inner	0	17,3	21,8	26,3
	Roll Distribution (%)		0	2,670	6,731	14,259
Rear Antiroll Bar	0	0	47,78	50,19	53,47	58,52
	Green - Soft	2,75	45,51	47,91	51,19	56,29
	Green - Mid	3,74	44,73	47,14	50,41	55,52
	Green - Hard	4,90	43,87	46,27	49,54	54,66
	Yellow - Soft	5,76	43,25	45,64	48,91	54,03
	Yellow - Mid	7,85	41,81	44,18	47,44	52,57
	Yellow - Hard	10,27	40,27	42,61	45,85	50,97
	Red - Soft	11,28	39,65	41,99	45,21	50,33
	Red - Mid	15,38	37,34	39,63	42,81	47,89
	Red - Hard	20,12	34,99	37,22	40,33	45,36

### 4.5 Mechanical Balance

This chapter about mechanical balance will show one of the main objectives of this tool to assist in deciding configuration changes. It corresponds to the springs, anti-roll bars and roll centres being adjusted taking into account the vehicle being in a stationary state when cornering. With this it is possible to have a support as a value, where it can be seen that the vehicle has a tendency to understeer or oversteer, however it also gives the support that in setup changes, such as springs, anti-roll bar or at different bar position must be considered to maintain the same mechanical balance as before.

Tarmac		Setup 1		Setup 2	
	Units	Front	Rear	Front	Rear
Ride Height	mm	103	115	103	115
Pitch		12		12	
Springs	N/mm	40	40	45	40
ARB		Yellow	Yellow	Yellow	Yellow
Position		Outter	Inner	Inner	Inner
ARB Stiff	N/mm	11,82	5,76	6,73	5,76

Figure 82 - Part of the cover tab at Excel software

With the notion of mechanical balance, and having defined the objective, so that the driver maintains the same feeling and balance in the car, with improved handling, let's look at an example. Figure 82 shows part of the Excel software coverage tab, where the surface considered is tarmac and there are two setups. Setup 1 is the base, or how the driver made the run, and setup 2 is the changes you want to make to the setup. The base change was the front spring from 40 N/mm to 45 N/mm, but by making just this change and keeping the anti-roll bars in the same position, the mechanical balance is different, in this example, the mechanical balance was 52.67%, rising to 54.61%, a difference of 2% with just the springs.

In order to maintain the same balance by changing the front spring, the front anti-roll bar needs to be moved to the inner position, so the mechanical balance will be 52.64%, which is very close to the initial configuration, as showed in Figure 83.

Rates			
Parameter	Units	Value Set1	Value Set2
Front tire rate	N/mm	300,00	300,00
Rear tire rate	N/mm	300,00	300,00
Front Spring rate	N/mm	40,00	45,00
Rear Spring rate	N/mm	40,00	40,00
Front Wheel rate (No ARB)	N/mm	26,30	29,59
Rear Wheel rate (No ARB)	N/mm	28,75	28,75
Front Ride Rate (No ARB)	N/mm	24,18	26,93
Rear Ride Rate (No ARB)	N/mm	26,23	26,23
Front ARB rate	N/mm	11,82	11,82
Rear ARB rate	N/mm	5,76	5,76
Front Spring + ARB Rate	N/mm	51,82	56,82
Rear Spring + ARB rate	N/mm	45,76	45,76
<b>Front Total Rate</b>	N/mm	44,19	47,77
<b>Rear Total Rate</b>	N/mm	39,70	39,70
		<b>52,67%</b>	<b>54,61%</b>

Figure 83 - Part of the mechanical balance tab at Excel software

It's in these decisions that this tool is very useful, because here we take a situation as an example to describe the problem and the solution. The test time for each event is limited and each run lost has not only the loss of time, but also the economic aspect. If we only change the springs, the driver will complain that he doesn't feel comfortable with the car and, for the expected value, the vehicle will be more understeered. If, on the next run, you change just one position of the front anti-roll bar, the driver will feel better, but won't have the same feeling as in the first configuration. And this is not only frustrating for the driver because time is running out and he doesn't have the car the way he wants it for the event, but he's still wasting time that could be used to make some changes if a situation arises during the race.

With this tool providing a value for the mechanical balance and other metrics to be analysed after the test day or event, it is a useful tool for every engineer to be more precise and accurate in their decisions.

#### 4.6 System Response Analysis

Chapter 2.13 Vibration System and Damper showed the damping ratio and the importance of the critical damping with  $\xi = 1$ , which responds most quickly to the settling of the damper at the zero point, and deviating from this value will affect the response.

With the mass of the vehicle, and the spring stiffness, it is possible to analyse the damping of the damper. This part is more for future analysis and to work on the damper, if possible, since when testing or race event, time is limited and it's not possible to analyse every aspect. There,

the focus is more on the mechanical balance for choosing changes in terms of setup of the vehicle.

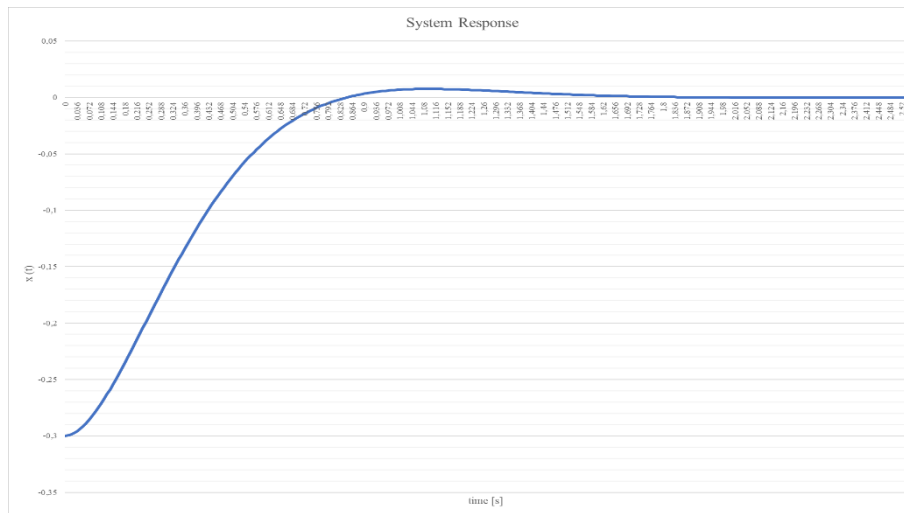


Figure 84 - System response for damping ratio 0.75

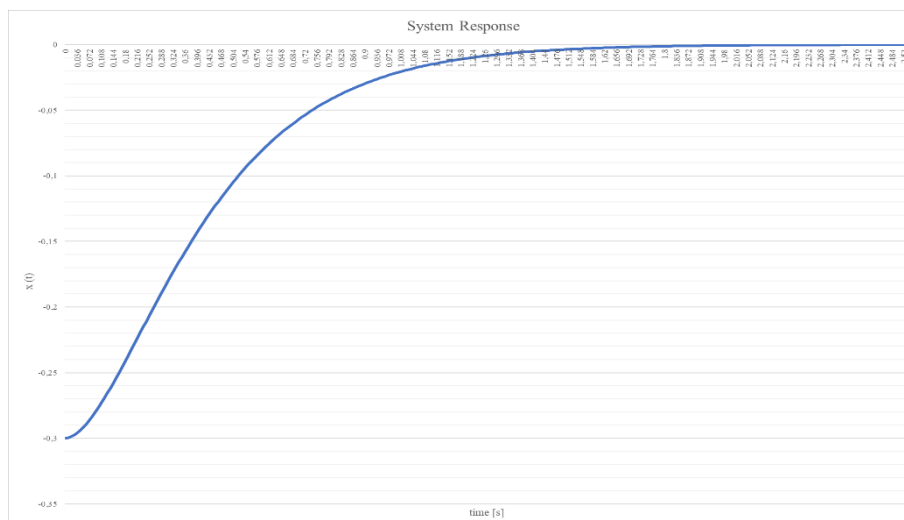


Figure 85 - System response for damping ratio of 1

Figure 84 and Figure 85 show the response of the system for different damping ratios.

The first conclusion, also explained in chapter 2.13 Vibration System and Damper, is that the damping ratio equal to 1, critical damping in Figure 85, causes the response to settle more quickly, which in this case is at 1,8 seconds. In contrast to the response of the system for a damping ratio of 0,75 in Figure 84, the response is 1,95 seconds. The difference is small but also necessary to identify the overshoot in this case, an undesirable situation.

### 4.7 Data Analysis

Data analysis, often mistakenly referred to as telemetry - telemetry consists of direct contact with the vehicle, which in the vast majority of cases is not done - is the reading process carried out, in the particular case of the Skoda Rally2, by means of the software patented by the manufacturer Magneti Marelli, Wintax, which is the interface to be used in the latest vehicles, as far as rally vehicles are concerned. In this sense, the software makes it possible to analyse issues such as the main oil, fuel and water pressures, engine, gearbox and differential temperatures, engine knocking and the driver's driving performance, among many others.

The aim of this chapter is to give you a brief insight into how the software works, starting by presenting the programme's interface, the data acquisition process, configuration examples and existing possibilities.

### 4.7.1 Wintax4 - 4.80

The graphic interface of Wintax 4.80, the software used to analyse the data, is very intuitive, with a predefined layout provided by Skoda Motorsport, in which each tab relates to a different analysis component, present in Figure 86. (Skoda\_Motorsport 2019)



Figure 86 - Wintax software interface

On the top panel of the software, the user must click on Acquisition, Figure 87, and after clicking, a series of steps will appear, such as identifying the name of the event, the driver name, the lap number, so that all the data that is successively added to the work computer can be stored in the most organised way possible, Figure 88. These steps may not be completed, but organising the information will make it easier to consult in the future, should the need arise.

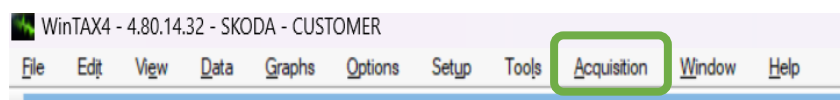


Figure 87 - Acquisition tab on Wintax

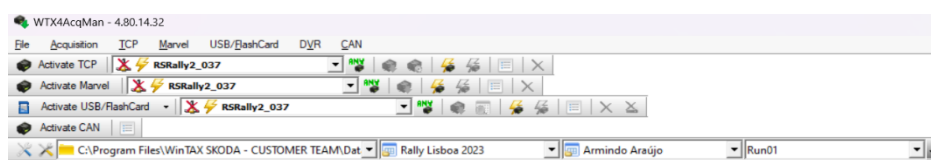


Figure 88 - Acquisition manager on Wintax

### 4.7.2 Analysing Data

Firstly, it is important to ensure that the vehicle is in good working order, forgetting for the moment the driving style that the driver will be using and the improvements to their driving. This is one of the main tasks of data analysis. Analysing engine pressure, temperatures, diagnostic errors, and many other factors, as shown in Figure 89, is crucial to the success of a

rally or any event, because, as you know, if something fails mechanically, the probability of failure is high.

These parameters are then analysed in a tab, in this case the Diagnostics tab, with the corresponding mathematical channels associated with the vehicle sensors that allow this type of value to be analysed.



Figure 89 - Interface with data for analyse in one stage

It should be noted that, despite its apparent complexity, as more events such as tests and rallies take place, the sensitivity to detecting possible errors/problems arises or preventive detection is greater. It turns out that this is typical engine behaviour in a race mode situation, with oil and water temperature values that are all common and quite acceptable.

This is just one of the tabs available for analysing the vehicle's sensors, where you can see the main aspects to analyse and quickly check if there are any errors or malfunctions. There are other tabs that analyse each factor in depth, such as the engine, temperatures, oil, knocking, gears and others that give a more in-depth analysis of the state of the sensors, corresponding to the state of the vehicle.

### 4.7.3 Driving Data

Another of the important issues associated with analysing data has to do with translating what is acquired from the graphical data into the driver's driving ability. In fact, this topic is so decisive and crucial to improving a driver's driving that it's increasing the concern of drivers, not only young ones but also those with years of experience, to understand where things are going wrong or where they can improve the way they drive and approach a particular corner or stretch of road. When this analysis is carried out and it is clear that the work that has been done has been perfected, such as formulas that are driven on a track, where the state of the track is mostly constant and the driver's knowledge evolves the more laps they drive, the correction of the driving has a noticeable impact on the final result.

However, the rally environment is not the same as that of a track, as the grip of the road changes from stage to stage, the approach to corners is constantly changing, as well as the various vehicles passing on the road can get dirty, all of which affects the driver's approach and driving. This doesn't mean that it's impossible to improve or correct, for example, the approach to a corner on the way to perfection. By analysing the data, you can see how much and harder a driver brakes when approaching a turn, the position of the steering wheel and how sharp he steers, the corrections he makes in the middle of the turn, among other aspects of driving.



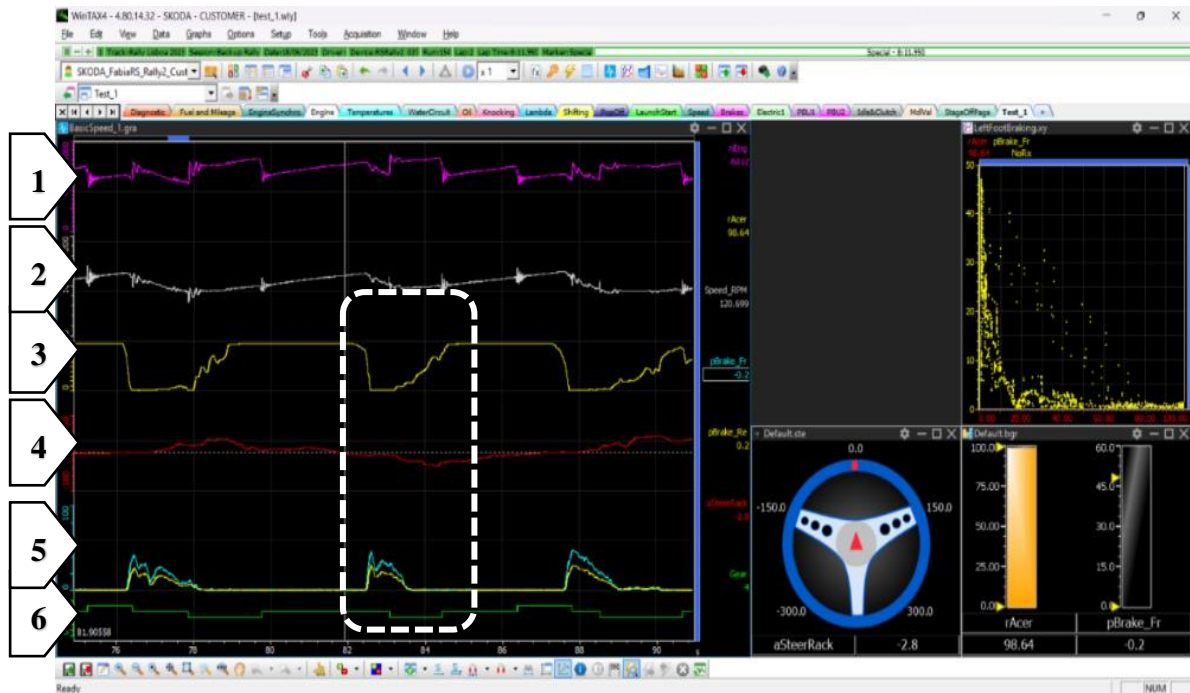


Figure 90 - Interface driving analyses

To understand and explain Figure 90, point 1 is the engine speed in rpm, point 2 is the vehicle speed, point 3 is the accelerator pedal position, point 4 is the steering angle, point 5 is the front brake pressure in blue and the rear brake pressure in yellow and point 6 is the current gear. On the right-hand side, at the top right, you'll find an x-z diagram of the left foot brake; below that, a simple bar graph window with the throttle position and front brake pressure and, on the right-hand side, as the picture shows, a representation of the steering wheel.

Looking at the signalling part, you can see progressive acceleration, almost without question, and good braking too with a quick change from the accelerator pedal to the brake pedal, which was 0.3 seconds, full braking at the start and after a tap of the brake pedal. This is an example that drivers should follow and work on improving their driving skills.

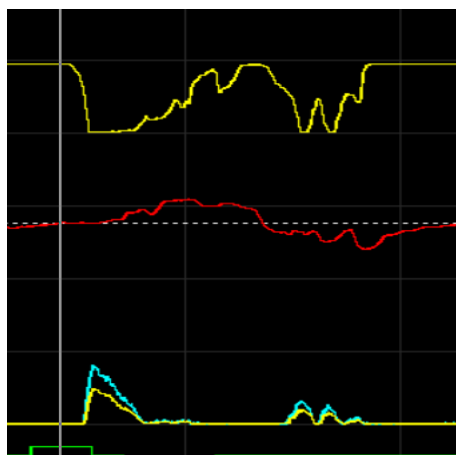


Figure 91 - Correction on the driving

Figure 91 shows an example of oversteer, hesitation on the accelerator pedal and some pressure on the brake pedal. In the case of the red line, as a steering angle line, it can be concluded that this is a right-hand corner. Firstly, you can see good braking for the lines at the bottom. From observation, when you start pressing the accelerator pedal while describing the

right-hand corner, at the exit of the corner it was necessary to correct the steering by turning it to the left, lift the accelerator pedal and also some pressure on the brake to correct the oversteer, with the line corrected the driver was able to fully depress the accelerator pedal and continue. Looking at this data alone, it is hypothesised that the driver pressed the accelerator pedal too soon, however, here it is not possible to know what the road was like, if there was any dirt or if the tyres were very worn, so it is important to analyse the data and discuss these points with the driver at the end of the stage to understand the cause of this correction, in this case as an example.

The software has the possibility of comparing two runs to see where it is better and if occur improvement or, on the other hand, whether the change is worse or better. In Figure 92 you can see two different runs made during the test session. The difference in terms of setup is that the run with the green colour as the yellow rear anti-roll bar in the outward position and the run with the red colour as the red rear anti-roll bar in the inward position, so it's a harder step for the rear in terms of setup. With the change to a harder step of the rear anti-roll bar it is expected that the vehicle will oversteer more, and this can be seen in the data, as shown in the figure. Note that in a right-hand corner, with the red anti-roll bar, the driver has to correct and steer to the left when exiting the corner, as can be seen in the image of the steering wheel, which corresponds to the right arrow. This was an experiment to stiffen the rear a little more to see how it felt and whether it could be an option for the event, but after this run the driver complains about oversteer and that the yellow rear anti-roll bar is the option for the event. Not only does it feel better, and the load transfer is more constant, but it also gives him more confidence.



Figure 92 - Comparison of data of two test runs



## 5 Conclusion and Recommendations

In order to carry out this final work and project, it was necessary to acquire new topics related to vehicle dynamics with a specific application to competition vehicles, with topics related to knowledge from previous years in the curricular units that were part of FEUP's master's degree in mechanical engineering. The process of carrying out this dissertation presented a very important challenge in relating all the information based on the bibliographical review that formed the base of this project with physical models close to reality, and access to more detailed information on some topics. It was a period in which the difficulties and challenges in the field of automotive competition were realised.

As part of the dynamic study, the foundations were acquired for future work on automotive motorsport, it was possible to understand the vehicle's behaviour in order to correct situations of understeer or oversteer, the influence of parameters on the vehicle's dynamics, the behaviour of the mechanical balance, the work of the dampers, or the influence of the tyres on the suspension system.

Based on the theory of automotive dynamics, a spreadsheet was developed using Microsoft Excel with the main objective of optimising the dynamic behaviour of a competition vehicle. The use of this tool, developed within the scope of this dissertation, will allow, in a more accurate way, to make changes to the vehicle's parameters in order to increase its efficiency. The analyses provided by this tool will allow changes to be made to the vehicle with greater confidence.

The developed tool is structured through a set of sheets as follows:

- **Cover:** the main spreadsheet, where the setup values are entered, and the most important values of the parameters needed for the decision are displayed, with the possibility of comparing two different setups.
- **Input data:** given the multiple variables required and the data needed for the calculations, this spreadsheet was created, where the input data values, and the values needed for the calculations are grouped together. In this way, the variables and the necessary data are organised in a single spreadsheet, simplifying future work.
- **Center of Gravity:** where the calculations for the location of the centre of gravity and the centre of gravity of sprung mass are calculated. This spreadsheet also calculates the height of the front and rear roll centre.
- **Spring:** where the wheel rate, spring frequency and spring anti-roll torque are calculated.
- **ARB:** where the different front and rear anti-roll bar ratios are calculated, with the necessary wishbone ratio being calculated so that the total rate can then be calculated. The roll distribution study is also presented, considering one of the front anti-roll bar positions in relation to the different front diameters and the different rear anti-roll bar diameters and positions.
- **Mechanical Balance:** with all necessary tyres, spring and anti-roll bar rates, the total rate can be calculated, and the mechanical balance calculated. This value is the key parameter to analyse when considering changes or seeking to change the vehicle's behaviour, taking understeer or oversteer into account and depending on driver feedback.
- **Weight Transfer:** for calculation how weight transfer occurs in the vehicle laterally and longitudinally. The calculations for lateral weight transfer are based on linear behaviour, which does not fully correspond to real behaviour, but it does give an idea of the weight transfer. For the longitudinal weight, it is necessary to consider the anti-dive and anti-squat effects in order to obtain more accurate longitudinal weight transfer values.

It was possible to test the developed tool during a test event, where the front springs had to be changed, but the balance had to remain the same, so the position of the front anti-roll bar was changed at the same time as the springs were replaced. With the changes made, the driver did the test section, and the feedback was positive, maintaining the same mechanical balance, although the handling improved, giving the driver more confidence and increasing performance. This is the strength of this tool, as the changes made to the setup maintain the mechanical balance, and in terms of efficiency in the matter of time. In other words, the test time is utilised more efficiently and there is the possibility of testing other changes and verifying whether or not there has been an improvement.

Developing this tool was a good way to put the theory into practice by visualising the various systems in the vehicle's behaviour, and how they relate to each driver's driving style and to optimise performance.

The realisation of this dissertation not only helps to understand the vehicle, but also to understand more deeply the work of a race engineer in the competitive world of vehicles. All the preparation before the week of the event to organise all the things on the vehicle. The pre-event of the rally to make the final changes in terms of setup and the real handling of the car in conditions similar to those encountered on the event weekend. The confirmation of things in the vehicle for the initial scrutineering to seal the car's components. The responsibilities during the event weekend, the contact with the driver and the feedback transmitted from the car, with the discussion to improve that feeling.

This work provided valuable knowledge of the engineering work carried out and the entire context and preparation that existed for the event. This practical knowledge was a different skill developed in this study and the understanding that not only theoretical components are needed, but also organisation, vehicle management, and the ability to adapt to different scenarios.

To continue the project developed for this dissertation, future work is proposed.

Firstly, the tool developed can be improved, with more precise dimensions and adding more features and parameters from the suspension system, more data from the tyres and from, the chassis.

A better study of torque and the transmission system that influences the suspension system is proposed, because if too much torque is applied, the wheel will spin, losing traction and influencing the vehicle's handling and dynamics.

Applying accelerometers and/or gyroscopic sensors to the vehicle during tests to record data on the forces acting on the vehicle, thus creating analysis measures, in order to have more metrics for optimisation. The more information collected on the vehicle's dynamics, the better the decisions and the more accurate the developed tool.

## References

- Balkwill, James. 2018a. "Braking." In *Performance Vehicle Dynamics*, edited by Elsevier Inc., 181-196. Matthew Deans.
- . 2018b. "Cornering." In *Performance Vehicle Dynamics*, edited by Elsevier Inc., 95-179. Matthew Deans.
- . 2018c. "Dynamic Modelling of Vehicle Suspension." In *Performance Vehicle Dynamics*, 241-317. Matthew Deans.
- . 2018d. "Tyres." In *Performance Vehicle Dynamics*, edited by Elsevier Inc., 11-52. Matthew Deans.
- Baylos, Hermenegildo. 2016. *Fundamentos Sobre Comportamiento Dinámico Del Coche Deportivo*.
- Beckam, Brian, ed. 1991. *The Physics of Car Racing*.
- Bugeja, Keith, Sandro Spina, and Francois Buhagiar. 2017. "Telemetry-based optimisation for user training in racing simulators." 2017 9th International Conference on Virtual Worlds and Games for Serious Applications (VS-Games).
- Catto, Christopher. 2012. "Damper.pdf>."
- Crahan, Thomas C. 2023. "Modelling Steady-State Suspension Kinematics and Vehicle Dynamics of Road Racing Cars\_Part I." *Journal of Commercial Vehicles (1996)* 105. <https://www.jstor.org/stable/44718244>.
- Ferreira, Pedro Paive e Fernando. 2023. "Cap4\_Centros instantâneos de rotação."
- Guiggiani, Massimo. 2018. *The Science of Vehicle Dynamics*.
- "Intercomp." <https://www.intercompracing.com/5000-lb-digital-coil-spring-tester-p-119.html>.
- Kasprzak, Jim. 2012. *A Guide To Dampers*.
- Michelin, Société de Technologie. 2001. *Michelin\_Tire\_Grip*.
- Rajamani, Rajesh. 2005. *Vehicle Dynamics and Control*.
- Rio, Pedro Jorge Ferreira Espinheira. 2009. "Dinamica e afinação de uma viatura de competição." Mechanical, FEUP.
- Rodrigues, José Dias. 2021. *Apontamentos de Vibrações de Sistemas Mecânicos*.
- Seward, Derek. 2014. *Race Car Design*.
- Skoda\_Motorsport. 2019. *WintAX4\_manual*.
- . 2023a. *A5777\_Skoda Fabia 1.0 MPI 55kW-1*.
- . 2023b. *RS-User\_Manual*.
- Smith, Carroll. 1978. *Tune To Win*. First Edition ed., edited by Carroll Smith Consulting: Aero Publishers, INC:.
- William F. Milliken, Douglas L. Milliken. 1995. *Race Car Vehicle Dynamics* edited by SAE International: SAE International.

## ANNEXE A: Data from Skoda

Table 15 - Springs available and homologated by Skoda for tarmac.

Tarmac			
Front		Rear	
Reference	Stiffness [N/mm]	Reference	Stiffness [N/mm]
<b>6VT411101 AA</b>	60	<b>6VT411101 AA</b>	60
<b>6VT411101 T</b>	55	<b>6VT411101 T</b>	55
<b>6VT411101 S</b>	50	<b>6VT411102 C</b>	45
<b>6VT411102 C</b>	45	<b>6VT411102 B</b>	40
<b>6VT411102 B</b>	40	<b>6VT411102 A</b>	35
<b>6VT411102 A</b>	35	<b>6VT411102</b>	30
<b>6VT411102</b>	30		

Table 16 - Springs available and homologated by Skoda for gravel

Gravel	
Front and Rear	
Reference	Stiffness [N/mm]
<b>6VT411101 AN</b>	37.5
<b>6VT411101 AM</b>	35
<b>6VT411101 AL</b>	32.5
<b>6VT411101 AK</b>	30
<b>6VT411101 AJ</b>	27.5
<b>6VT411101 AH</b>	25
<b>6VT411101 AG</b>	22.5
<b>6VT411101 AF</b>	20
<b>6VT411102 J</b>	17.5
<b>6VT411102 H</b>	15

# ANNEXE B: Worksheet

Cover

Input Data

CG

Mechanical Balance

Spring

ARB

Damper

Diferential

Weight Transfer

Tarmac		Setup 1		Setup 2	
	Units	Front	Rear	Front	Rear
Ride Height	mm	103	115	105	115
Pitch		12		10	
Springs	N/mm	40	40	45	40
ARB		Yellow	Yellow	Yellow	Yellow
Position		Outter	Inner	Inner	Inner
ARB Stiff	N/mm	11,82	5,76	6,73	5,76
Wheel Rate [no ARB]	N/m	26298,05	28745,56	29585,31	28745,56
Ride Rate [no ARB]	N/m	24178,55	26232,05	29013,07	28338,26
	%	48%	52%	51%	49%
Suspension Roll Stiffness	Nm/deg	1,17	1,03	1,17	1,03
Spring + ARB Rate	N/m	51817,64	45757,24	51731,30	45757,24
Ride Rate	N/m	44185,65	39701,76	50006,69	44733,79
	%	52,67%		52,78%	
Roll Stiffness	°/G	4,08		3,60	
Rolling Percentage	%	11,7%		-13,2%	
Pitch Angle	°/G	0,20		0,18	
Diving	%	47,3%		47,2%	
Roll Rate	Nm/rad	57337,98	51200,11	37649,11	36545,53
Differential Ramps		44	44	44	44
Friction Faces		16	8	16	8

**Acceleration Lock**

Locking Front: 68,10%

Balance: 66,67%

Overall: 51,07%

Rear: 34,05%

44/85 16FF 44/85 8FF

**Acceleration Lock**

Locking Front: 68,10%

Balance: 66,67%

Overall: 51,07%

Rear: 34,05%

44/85 16FF 44/85 8FF

**Deceleration Lock**

Locking Front: 5,75%

Balance: 66,67%

Overall: 4,32%

Rear: 2,88%

44/85 16FF 44/85 8FF

**Deceleration Lock**

Locking Front: 5,75%

Balance: 66,67%

Overall: 4,32%

Rear: 2,88%

44/85 16FF 44/85 8FF

Figure 93 - Excel cover spreadsheet

## ANNEXE C: Recording Measurements

### Mesures

Roll Centre			
Parameter	Units	Fr Value	Rr Value
AB	mm		
AC	mm		
BG	mm		
ED	mm		
EF	mm		
Angle	°		
<b>Notes:</b>			

Spring Installation Rate			
Parameter	Units	Fr Value	Rr Value
d1	mm		
d2	mm		
Damper Angle	°		
<b>Notes:</b>			

ARB Ratio			
Parameter	Units	Fr Value	Rr Value
Inner	mm		
Middle	mm		
Outer	mm		
<b>Notes:</b>			

Car			
Parameter	Units	Fr Value	Rr Value
Track	mm		
Wheelbase	mm		
<b>Notes:</b>			

Figure 94 - Measurement record sheet